The Nature Conservancy

GEOSPATIAL ANALYSIS OF FOREST CONDITION AND CONNECTIVITY IN THE NORTHEAST U.S.

February 4, 2025

The Nature Conservancy, Center for Resilient Conservation Science

For more information, online maps, and datasets visit our website at: https://crcs.tnc.org/

Explore the Results and create area based reports at:
https://www.maps.tnc.org/neforestcondition

Please cite as: Clark, M., M. G. Anderson. 2024. Geospatial Analysis of Forest Condition and Connectivity in the Northeast U.S. The Nature Conservancy, Center for Resilient Conservation Science.

This project was supported by the Northeastern States Research Cooperative through funding made available by the USDA Forest Service. The conclusions and opinions in this paper are those of the authors and not the NSRC, the Forest Service, or the USDA.

About the Cover:
Burnt Mountain, VT © Eamon Mac Mahon. Looking towards Burnt Mountain, Vermont, from the north. Burnt Mountain was acquired by TNC in 2018. It is approximately 5,500 acres along Vermont's northern border and currently the largest natural area amongst TNC's 55 Natural Areas. Intact, connected, and healthy forests such as this clear air, remove pollutants, improve water quality, and slow the pace of climate change through carbon sequestration.

Table of Contents

Figures and Tables

Abstract

To ensure the long-term sustainability of the Northern Forest, land managers, agencies, and conservationists need a way to measure and monitor forest condition, assess how it is distributed across the region, and estimate the impact of forest management practices. Identifying areas where forests are improving or degrading, understanding the prevalent condition, mapping the most climate-resilient sites, and determining how individual management decisions influence landscape connectivity are essential steps in this process. Fortunately, the last decade has seen considerable progress in the creation of consistent, remotely sensed, time-series datasets that through careful processing and interpretation can be the basis for a new generation of spatially explicit, dynamic maps depicting forest condition.

In this project for the Northeast States Research Cooperative, we assessed geospatial and remotely sensed data on forest condition and used three derived metrics to model connectivity to support species range shifts. The three forest condition factors that we identified as consistently and accurately mapped throughout the region were 1) forest age/forest height, 2) forest turnover, and 3) lack of human disturbance. We validated the data for each of these factors using Forest Inventory and Analysis (FIA) data to ensure our models were representing characteristics of the forests also identified on the ground. We assessed each factor individually and then integrated them into a Geospatial Forest Condition Index. Next, we measured forest connectivity using the forest condition factors in combination with other resistance inputs. Our aim was to estimate connectivity to support species range shifts where the condition of the forest could influence establishment and survival. We found that the tallest forests in the region are Central Oak Pine forests at an average of 19.9 meters, followed by Northern Hardwood & Conifer at an average of 18.6 meters. Boreal Upland Forest had the lowest average height of 14.4 m. At a regional scale we found that the Boreal Upland Forest had an average turnover rate of 80,000 acres per year or 0.7 % of the forest type, which was over twice more than Northern Hardwood and Conifer Forest (0.27%/year) or Central Oak-Pine (0.07%/year). In contrast the degree of human disturbance from roads, had the reverse distribution with Central Oak-Pine scoring below-average (-0.2 SD), Northern Hardwood and Conifer slightly-above-average (>0.5 SD) and Boreal Upland Forest far-above-average (1.1 SD) compared to the average for forest in the region. In the integrated condition metric Northern Hardwood and Conifer Forest was the only forest type that scored above the mean although all three forest types were close to the mean of the region (0 in z-score) highlighting the importance of this habitat to the Northern Forest. For connectivity for range shifts, Boreal Upland Forest had the highest connectivity and also had the highest potential for improved connectivity with improved management. We calculated all metrics at both the regional and local scale and integrated the results into a user-friendly decision support tool aimed at decision makers and other concerned audiences. The tool allows users to zoom into each forest types and find specific areas that score higher or lower. We hope the results and the tool will allow users to explore and better understand the dynamic condition of the Northern Forest and make informed decisions about the individual and cumulative impact of various management activities.

Introduction

The Northeast Forest, covering much of New England and New York, is part of the largest remaining contiguous patch of temperate forest in the world, and is known for its scenic beauty and distinctive spruce-fir and northern hardwood forests. Land ownership in the region is a mosaic of industrial forest land, conservation lands, multi-use state forests, and private woodlots. With over 80% of the land in private ownership, including over 12 million acres in commercial enterprises, it is the quintessential working forest landscape (Nelson et al. 2010). The region still retains much of its natural character, most of its flora and fauna, and many of is characteristic mammals, although wolves, cougar and woodland caribou are no longer present. However, because the forest is managed by a wide range of private and public ownerships, it is difficult to assess the collective and cumulative impact of all the varying uses and landowner priorities, or to comprehend the range and spatial distribution of forest conditions. This makes it challenging to predict how land management practices will impact species and ecosystems that need to move or change in response to a changing climate, or how those practices affect the forest's life sustaining functions like natural filtration, production of clean air and water, and carbon sequestration and storage to mitigate climate change (Small & Lewis, 2010).

To ensure the long-term sustainability of the Northeast Forest, land managers, agencies, and conservationists need a way measure and monitor forest condition at a large scale, assess how condition is distributed across the region, and estimate the impact and benefits of forest management practices. Fortunately, the last decade has seen considerable progress in the creation of consistent remotely sensed, time-series datasets that through careful processing and interpretation could lead to a new generation of spatially explicit, dynamic maps depicting changes in geospatial forest condition.

For the Northeast Study Area (Figure 1) we:

- Compiled spatially-explicit metrics on forest age and height, turnover rates, degree of permanent conversion, and fragmentation from anthropogenic disturbance
- Validated the metrics with FIA data
- Developed an integrated, geospatially-based estimate of forest condition.
- Estimated the degree of forest connectivity available to support the movement and range shifts of forest dwelling species at two scales (local and regional).
- Identified areas where improving geospatial forest condition could have the largest improvement in connectivity at a local and regional scale.

Our goal in this project was to assess and synthesize geospatial information on forest condition, report on our findings, and translate them into a user-friendly decision support tool aimed at decision makers and other concerned audiences. The results will allow users to explore the condition of the forest at various scales and make informed decisions about the individual and cumulative impact of some management activities. This document provides the description, justification, and methods for the datasets in the decision support tool.

Forests in the Study Area

The focus of this study is the Northern States Research Cooperative (NSRC) states of New York, Vermont, New Hampshire, and Maine. However, because connectivity models rely on a larger analysis area to model current flow into and out of the system, we extended the analytical area to include the other New England states and parts of Canada (Figures 1 & 2). While condition attributes are mapped outside of the NSRC states, the models and weighting are for the NSRC states and the extended analysis area.

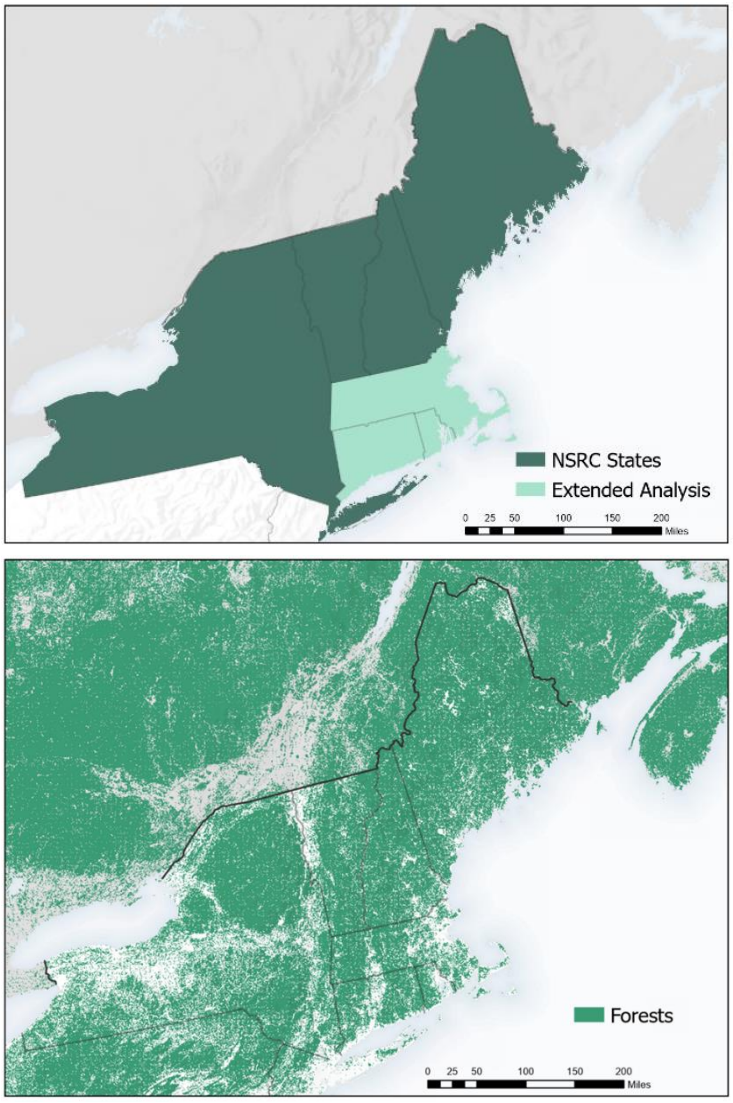

Figure 1: Study Area and extent of Northern forests.

We defined forest as any tree-dominated landscape, recognizing that they often experience disturbances, forest management activities, and other temporary vegetation changes. Stands that have undergone recent changes in surface vegetation due to a disturbance such as wildfire or harvesting, but that are expected to regain forest cover over a relatively short period were considered forest. Specifically, in the 2021 National Landcover dataset (Dewitz & USGS, 2023) we considered deciduous forests, evergreen forests, mixed forest, and woody wetlands to be currently forested land cover, and the category shrub-scrub could reflect forests in turnover. For Canada, we used the 2020 Landcover of Canada dataset (CCRS, 2020) for landcover and for current forest we used the temperate or sub-polar needleleaf forest, sub-polar taiga needleleaf forest, temperate or sub-polar broadleaf deciduous forest, and mixed forest but as the data does not separate woody wetlands and herbaceous wetlands, we excluded wetlands from our forest classes. To identify forest types for characterization and stratification, we used a finer-scale model of habitat types by macrogroup as mapped in the Northeast Terrestrial Habitat Map (NETHM, Figure 2) (Ferree & Anderson, 2013). The terrestrial and wetland habitats defined and described in the NETHM follow the Northeast Terrestrial Wildlife Habitat Classification (Gawler, 2008), with modifications as necessary to enable consistent mapping in the Northeast. The NETHM is a comprehensive and standardized representation of natural habitats across fourteen states and four Canadian provinces. Macrogroups based on a classification developed by NatureServe that define broad groupings of similar habitats.

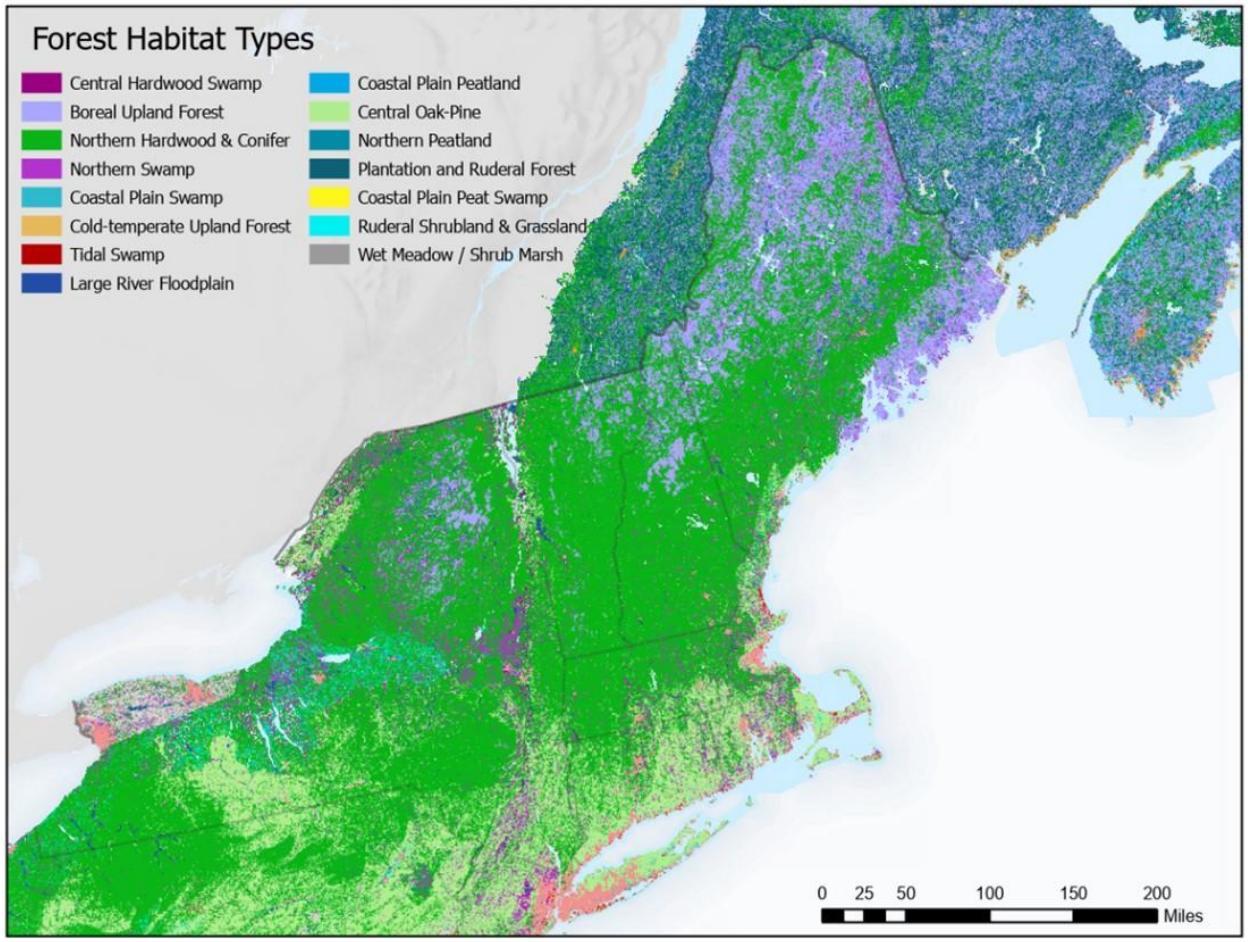

Figure 2: Forest Habitat Types by Macrogroup.

Estimating Forest Condition

There is a growing number of studies that attempt to map forest condition at large scales (Grantham et al., 2020), but there is no simple and widely recognized metric for assessing forest condition. Perceptions of quality and condition can vary greatly depending on which forest characteristics the observer values most and which temporal or spatial scales they used as criteria. Incorporating habitat condition information into conservation planning, however, can improve the outcomes of conservation by providing information on whether a particular site is likely to support focal species and healthy ecosystem function (Knight et al., 2010). Additionally, high condition forests can provide many benefits including carbon sequestration, clean water supply, and biodiversity (Grantham et al., 2020).

While there is no consensus of the definition of forest condition, characteristics of a forest in good condition can include (Kosiba, 2023):

- multiple tree species present,
- vertical complexity (trees of different sizes and ages),
- horizontal complexity (irregular gap, downed deadwood, and standing dead trees),
- lack of pests and pathogens, few invasive species,
- large patch sizes with few anthropogenic fragmenting features,
- quick recovery from disturbance.

In recent years, easily accessible satellite imagery and new analytical approaches have improved our ability to detect some of these characteristics or their proxies, and thus map and monitor forest extent at much larger scales. Limitations of remote sensing products include a coarse resolution and constraints on what can be detected. With these limits in mind, we sought to identify characteristics of the forest that were indicative of condition (or proxies that could be used to infer condition) that could be consistently and accurately quantified using remote sensing. After testing a wide variety of data, we found three factors met these criteria: forest turnover, tree age and height, and anthropogenic disturbance. We expected that we would be able to map other factors such as horizontal complexity, but we were unable to document strong repeatable relationships between the available datasets and our on-the-ground training data quantifying condition characteristics. Below we present our validation approach and the concepts and data sources for measuring each of the three factors.

Remote sensing data provides wealth of opportunities for consistent data and continuous data on forest condition. We wanted to make sure that the data we used to build our models actually represented characteristics of the forests on the ground. Our goal was to restrict the analysis to accurate and reliable data capable of supporting forest management land protection decisions.

Our validation methods are based on Forest Inventory and Analysis (FIA) data which provides an "unprecedentedly high-quality, consistent and systematic dataset" (Zhou et al., 2013). FIA is a nationally consistent, plot-based survey of America's forests containing roughly 125,000 plots nationwide. The consistent nature of the FIA sample design and its national sampling intensity of approximately one plot per 2,400 forested hectares, provides a unique view of forest plots across space and time (Bechtold & Patterson, 2005). The design for FIA inventory plots consists of four 7.3 m fixed-radius subplots spaced 36.6 m apart in a triangular arrangement with one subplot in the center that are measured once every 5–7 years in the eastern U.S. (Bechtold & Patterson, 2005). FIA plot samples contain a wealth of measurements; some examples include tree species, tree diameter, forest disturbance, forest type, and forest age (Hoover et al., 2022). Spatially, the FIA program fuzzes and swaps the precise locations to protect privacy landowner information. Fuzzing involves creating a buffer area of 0.5 to 1.0 miles around each plot and randomly selecting a point within that circle as the "new" coordinate for that plot (LaPoint, 2005). The FIA points are also swapped by exchanging plot coordinates for similar plots in the same county. In our validation, all of our calculations and statistics are neighborhood based to match the scale of the fuzzing.

Forest Condition Attribute 1: Forest Turnover

New England has a large forest product industry that includes forestry, logging, paper manufacturing, wood energy, and Christmas tree farming. In 2017, the forest product industry provided 62,599 jobs and 13.5 B in economic output (Holland & Meyer, 2018). The industry has a measurable impact on forest conditions with 6% of New England and New York forests (3 million acres) being logged, cleared, or destroyed by natural disturbances and then returning to forest over the last 20 years (Anderson et al., 2023). During that same period 0.5% of the forest was converted to development or agriculture, a conversion rate of 10,000 acres per year.

When forests are cut or removed it not only affects the stand itself but the disturbance releases resources allowing understory species and saplings to increase their growth. At small scales this can increase the vigor of the forest and allow more light to penetrate for forest floor, while at large scales extensive tree removal can disrupt the ecosystem, shifting the microclimates, drying the soils, and

allowing for the introduction of pests and pathogens. Slow rates of forest turnover may have neutral or positive effect on forest dwelling species, while high rates of turnover can make it harder for species to breed and raise young, or locate suitable habitat. Processes like erosion and water percolation and drainage may also be disrupted in areas subject to extensive and repetitive forest cutting.

To measure the distribution of forest turnover and conversion we used the Global Forest Change Project's high-resolution data on forest cover change (Hansen et al., 2013). In the dataset, forest turnover is expressed as a state change of a 30-m cell from a forest to non-forest to forest over a given time period. The product was developed by an analysis of Landsat images between 2000 and 2023 and has an annual time-step (Figure 3). We used the dataset to calculate the amount of forest turnover in a 1000-acre circular search area around each 30-m cell over the 22-year period (Figure 4). For the first Forest Condition Attribute, we used change within a 1000-acre circle (Figure 4), which is roughly equal to the size of the fuzzing of the locations of forest plots used by USFS's Forest Inventory and Analysis protocol. For this study, we defined stable forest as those where canopies were not removed between 2001 and 2023 (Figure 3). Stable forests were given the highest condition score with decreasing condition with increased turnover in the 1000-acre circle.

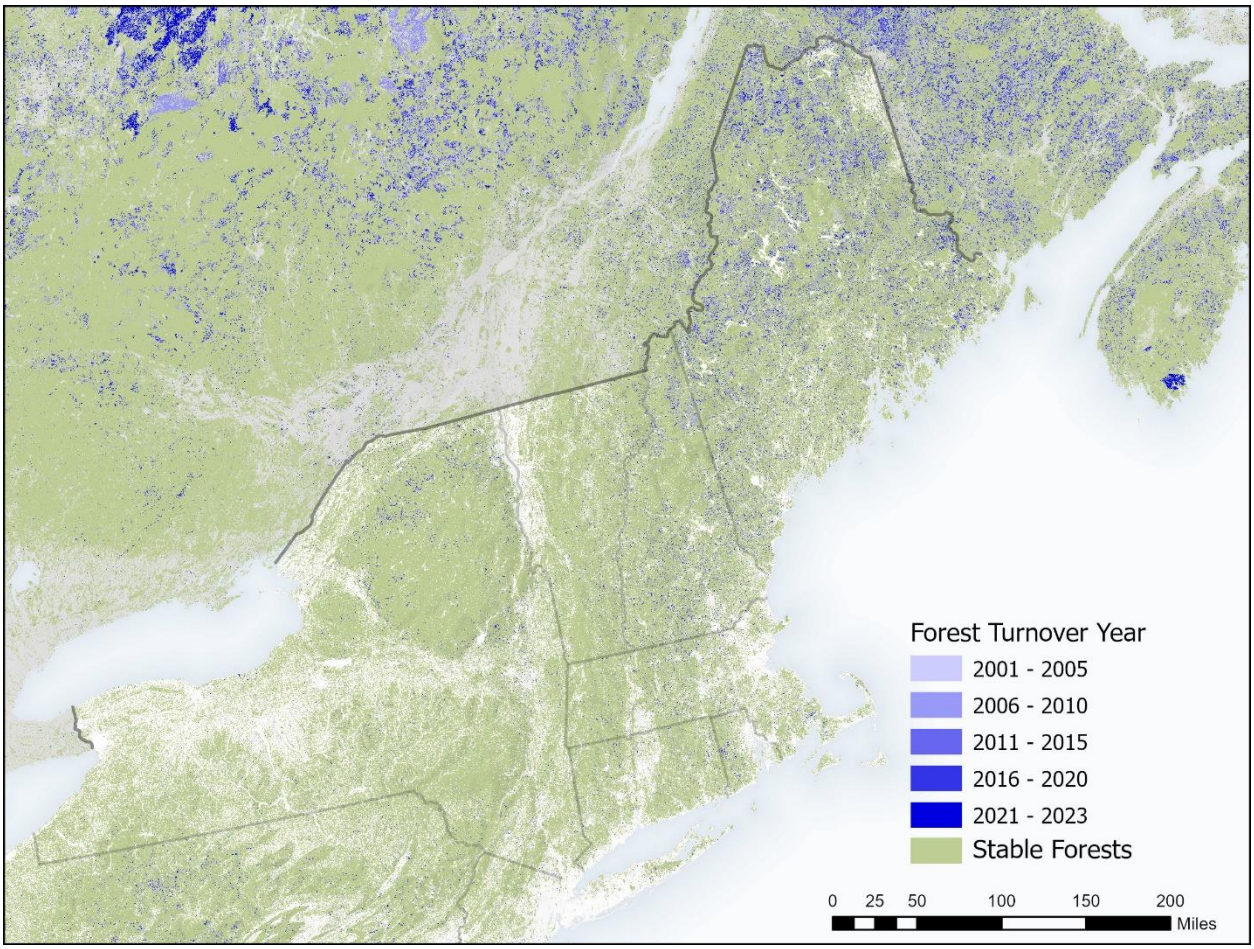

Figure 3: Forest Turnover from 2001-2023. This map shows the 30-m cells that changed from forest to non-forest during the 22-year period (Hansen et al., 2013).

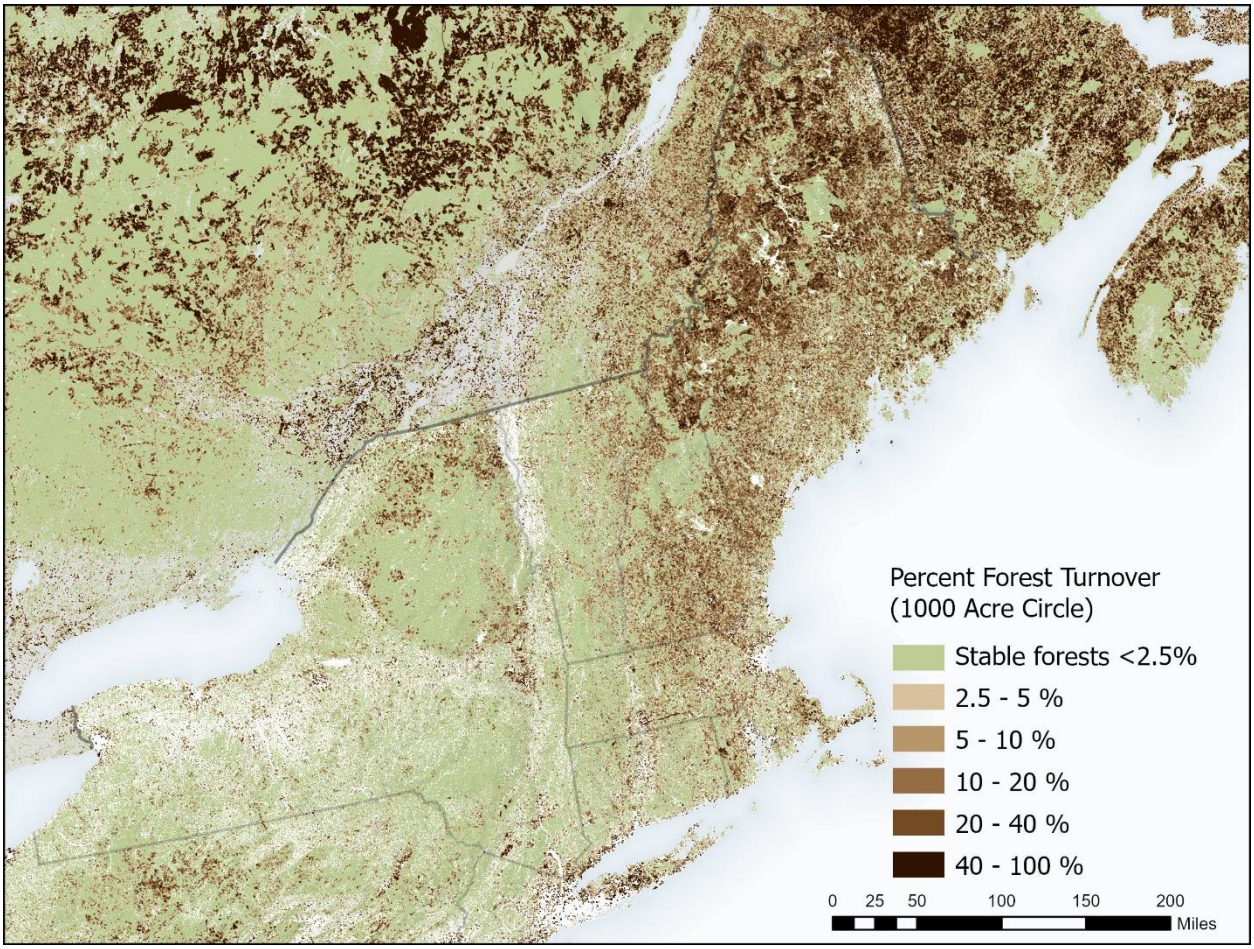

Figure 4: Percent Forest Turnover by 1000-acre Circle. This map shows the percent of forest turnover in a 1000-acre circular search area around each 30-m c . ells during the 22-year period from 2001–2023.

Validation of Forest Turnover

We validated the forest turnover dataset using two measurements from the FIA dataset: one at the plot scale and one at the tree scale. In the FIA dataset, the plot is the summarized unit of the survey location. Each plot is 2.5 acres (1.0 ha) in size and represents about 6,000 acres (2,428 ha) of land within a hexagon (Bechtold & Patterson, 2005). According to the FIA plot condition table, in our study area 1,479 plots were cut since 2000, and 3,278 had no cutting (Figure 5).

To validate the forest turnover data, we compared the average percent forest turnover in the FIA cut plots to those of the uncut plots. Cut plots had an average of 12.72% turnover per 1000 acres using the remotely sensed data while uncut forests have an average of 4.95% turnover per 1000 acres. These differences were significant using Kolmogorov-Smirnov test (P value <0.0001). Similarly looking at tree level data, of the 3,221 plots that had no tree removals after 1999, their mean percent turnover was 5.19% per 1000 acres. Of the 1,616 that had removals after 1999, their mean percent forest turnover was 11.68% per 1000 acres. These differences were significant using Kolmogorov-Smirnov test (P value <0.0001).

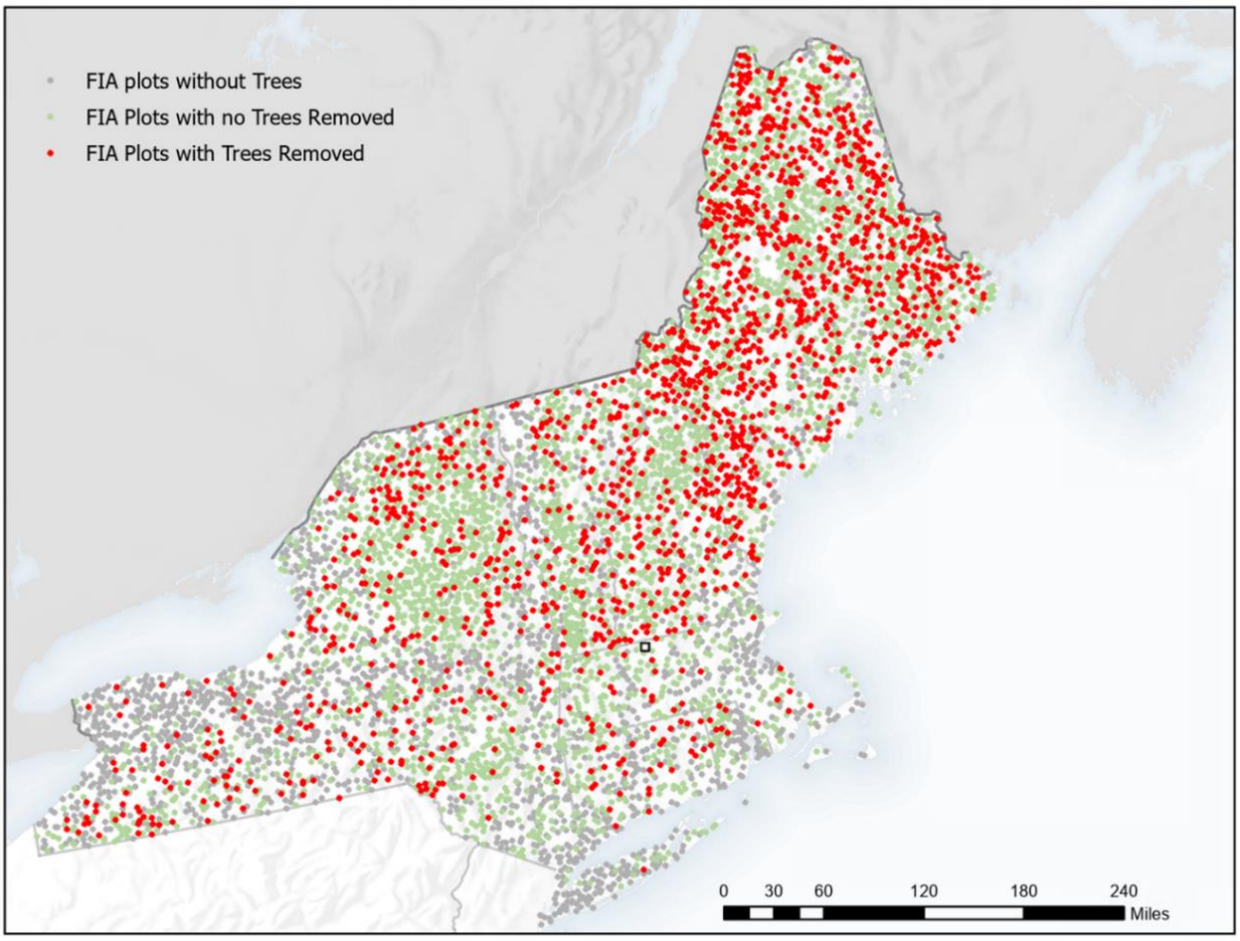

Figure 5: Location of the FIA plots used to validate Forest Turnover.

Forest Condition Attribute 2. Forest Height

Forest height is correlated with the age and growth rate of trees and can serve as an analog for the maturity of the forest, though it is less useful in distinguishing between tall stands of trees of moderate age and truly old, multi-generational forest stands. Older forests have more complex structures and develop more diverse and productive wildlife communities, while young forests often support a distinct community of early successional species. The age of the trees in a forest can provide an estimate of the amount of time since a stand-replacing disturbance event has occurred, such as a hurricane or a timber harvest. The metric has been used, in conjunction with other information to estimate productivity, carbon stock, and sequestration ability.

To quantify the distribution and variation in the height and age of the region's forests we use the Global Forest Canopy Height dataset (Potapov et al., 2021) which used the NASA GEDI, a spaceborne lidar instrument, to estimate forest canopy height in 2019 at a 30-meter scale. The map illustrates areas of short or recently cut forests in northern Maine that contrast with taller, older forests in the Adirondack mountains (Figure 6).

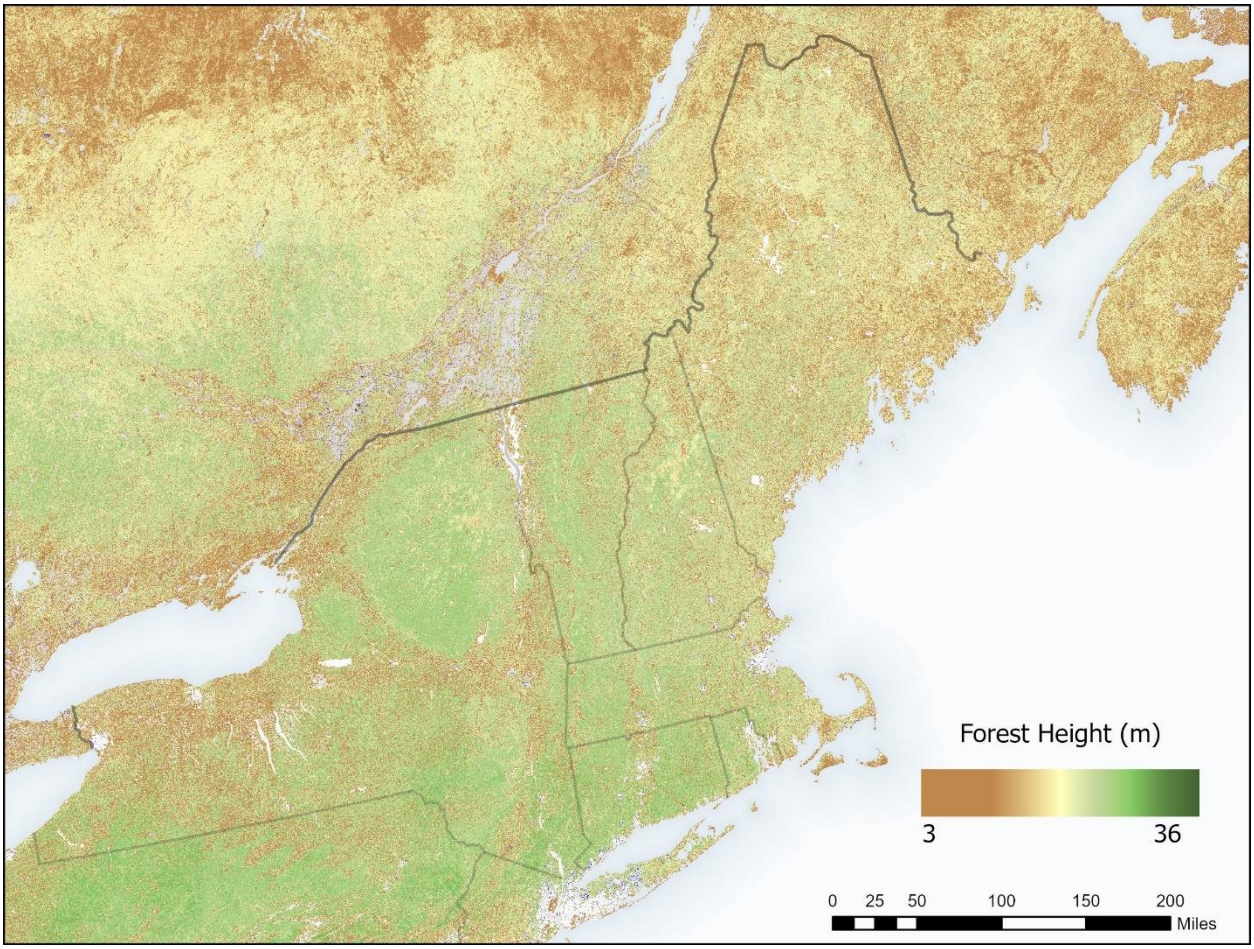

Figure 6: Forest Height. The forest height as detected by the GEDI satellite for northeast forests ranges in height from 3 meters (brown) to 36 meters (darkest green).

Individual tree species have different growth trajectories, and this leads to different forest types having different age-height relationship reflecting their composition and environments. For instance, northern conifers like spruce and fir have slower growth rates and persist in cooler environments compared to the oaks and maples of southern New England. To incorporate forest type, we overlayed the Northeast Terrestrial Habitat Map (Ferree & Anderson, 2013) forest height map and stratified the results by broad forest types using the NatureServe macro-groups (Figure 7 and Table 1). Within each type, we scored the highest condition to the tallest forests with condition decreasing as forest height decreases. We calculated the mean height for each type and converted the results to standard normal distributions (Z-scores). Canadian areas outside of the habitat map extent (grey area in Figure 7) were Z-scored relative to all forests. The resulting map (Figure 8) represents the distribution of tree heights within each of the forest types relative to the mean height of that habitat type.

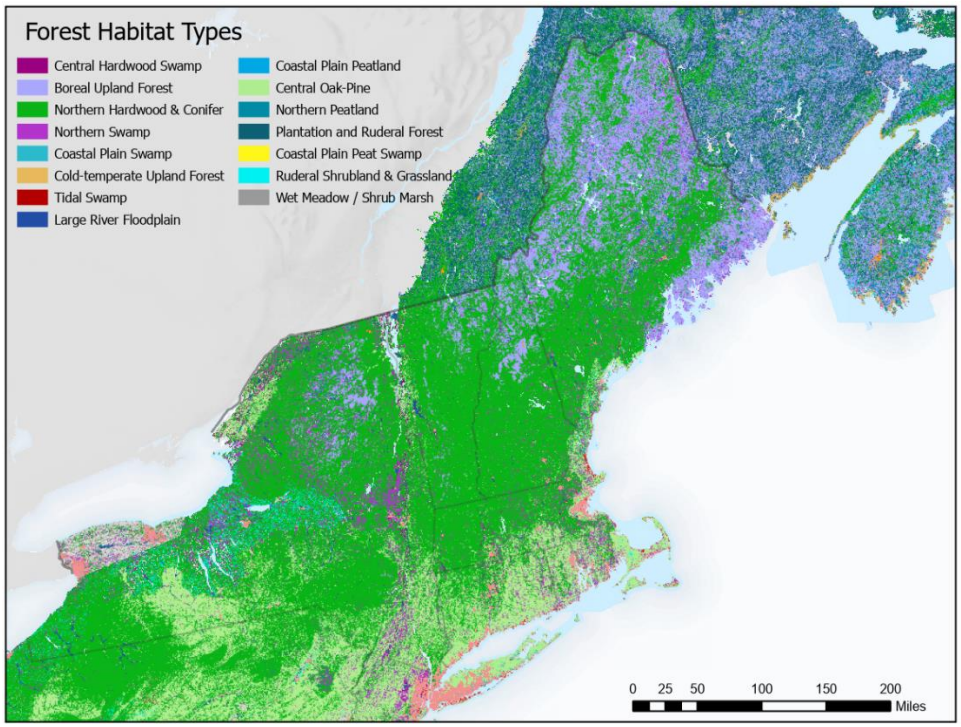

Figure 7: Forest Habitat Types. This map shows the region's 15 forest habitat types (macro-groups).

Macro-Group in Study Area	ACRES IN STUDY AREA	MEAN FOREST HEIGHT	STD FOREST HEIGHT
Northern Hardwood & Conifer	31,578,102	18.62	4.90
Boreal Upland Forest	7,668,280	14.04	4.60
Central Oak-Pine	4,802,460	19.91	5.13
Northern Swamp	3,965,355	16.25	5.59
Wet Meadow / Shrub Marsh	700,878	13.73	6.20
Large River Floodplain	555,872	14.37	5.78
Northern Peatland	456,546	11.30	5.67
Ruderal Shrubland & Grassland	336,413	16.89	6.46
Central Hardwood Swamp	152,324	16.24	5.92
Coastal Plain Peat Swamp	17,732	18.28	4.87
Coastal Plain Swamp	15,344	17.55	5.24
Tidal Swamp	904	16.56	5.78
Coastal Plain Peatland	884	13.68	5.97
Plantation and Ruderal Forest	745	14.26	5.33
Cold-temperate Upland Forest	37	11.14	5.06
Macro-Groups included for Connectivity			
Southern Oak-Pine	0	21.23	4.64
Southern Bottomland Forest	0	19.13	5.44
Boreal Forested Peatland	0	8.26	3.26
Cold-temperate Wet Forest	0	10.91	2.97
Central Oak-Pine/Longleaf Pine	0	16.23	4.94

Table 1. Acres and average height of the Forest Macro-Groups in the study regions. This table shows the acres of each habitat type and the mean and standard deviation of height in meters.

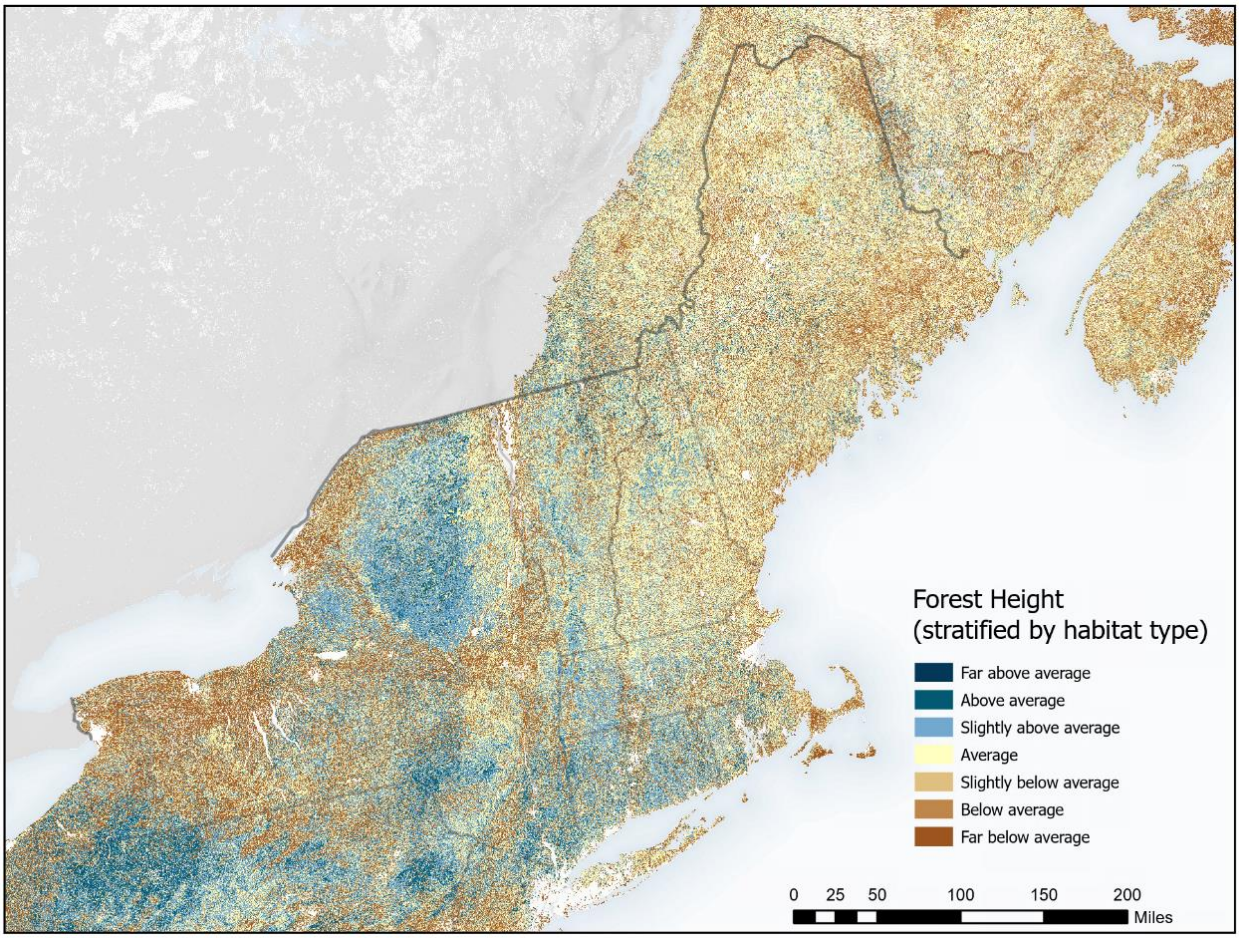

Figure 8: Forest Types by Height. The map shows the distribution of tree heights within each forest type relative to the mean height of the type.

Validation of Forest Height

To validate the forest height data we used two FIA data attributes: stand age and average height of live trees. Due to the "fuzzed" location of the FIA data, we compared these to the average height from the remote sensed data in a 1 km radius around the fuzzed point. Of the 6,661 FIA records 4,792 had live trees. We found that the forest height data was somewhat correlated with the FIA forest age ($r = 0.34$) and more strongly correlated with forest average height ($r = 0.60$).

The FIA data confirms differences in height between forest types (ANOVA, $P < 0.001$) with spruce-fir (boreal upland) habitats significantly shorter than oak-pine or white/red pine (central oak-pine) and maple-beech-birch (northern hardwood) intermediate between the two (Figure 9). The data also confirm differences in age (ANOVA, $P < 0.001$) although these are less pronounced. Aspen-birch (early successional) map as the youngest while oak-pine and maple-beech-birch map as the same age (Figure 9). These suggest that the analysis of height by forest type (Figure 8) is an appropriate way to interpret and display this data.

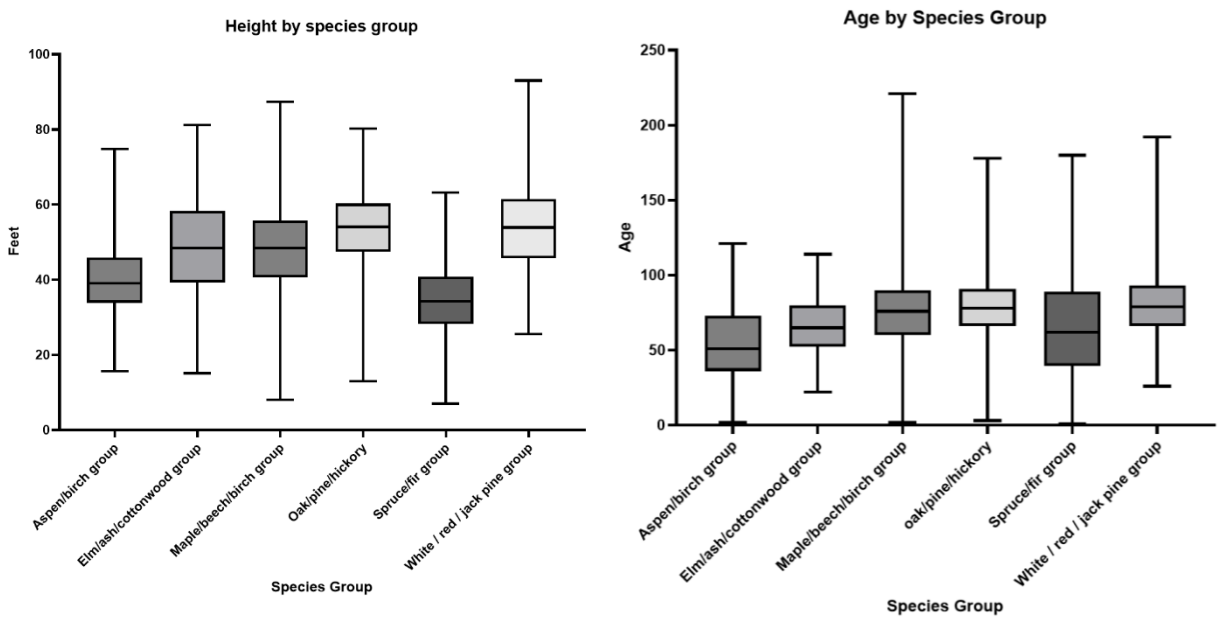

Figure 9: Forest Height and Age by species group in FIA data. The data shows the mean and box plot of height and age from the FIA sample data, arranged by FIA species groups.

Condition Attribute 3: Lack of Human Disturbance

Human activities can have a large impact on forest condition. Development and other forms of permanent conversion reduce the total amount of forest habitat while pesticide and herbicide applications decrease the quality of the existing habitat with respect to the plants and wildlife they sustain. Fragmentation by roads has been found to be particularly problematic. Road networks fragment existing species populations, amplify mortality in mammals and amphibians through vehicle-collisions, facilitate the spread of invasive species, increase noise, and facilitate soil compaction and erosion (Forman, 2003; Magioli et al., 2019; Mikołajczyk & Nawrocki, 2019; Trombulak & Frissell, 2000). The effects of roads extend a substantial distance into the forest, decreasing the amount of forest interior habitat available for breeding, and increasing accessibility in general (Avon et al., 2010; Lynch & Whigham, 1984). The “resistance grid” described below for modeling connectivity, includes all the fragmenting features found across the northeast forests, but here we give special attention to roads because their linear nature makes it easy to underestimate their effects.

We measured road density at two different distances: 5 kilometers for major roads (e.g. multi-lane highways, interstate highways), and 1 kilometer for all other roads. To map roads in the U.S. we used the US Census Bureau’s Topologically Integrated Geographic Encoding and Referencing system (TIGER) road dataset and in Canada we used OpenStreetMap roads (Geofabrik, 2022a; U.S. Census Bureau, 2023). In a few places we spot checked, the TIGER dataset did not appear to be comprehensive for dirt roads, so we augmented the dataset with dirt roads from OpenStreetMap. Major and minor road density grids were z-scored with respect to the study area and averaged together to create one spatial metric of road density (Figure 10).

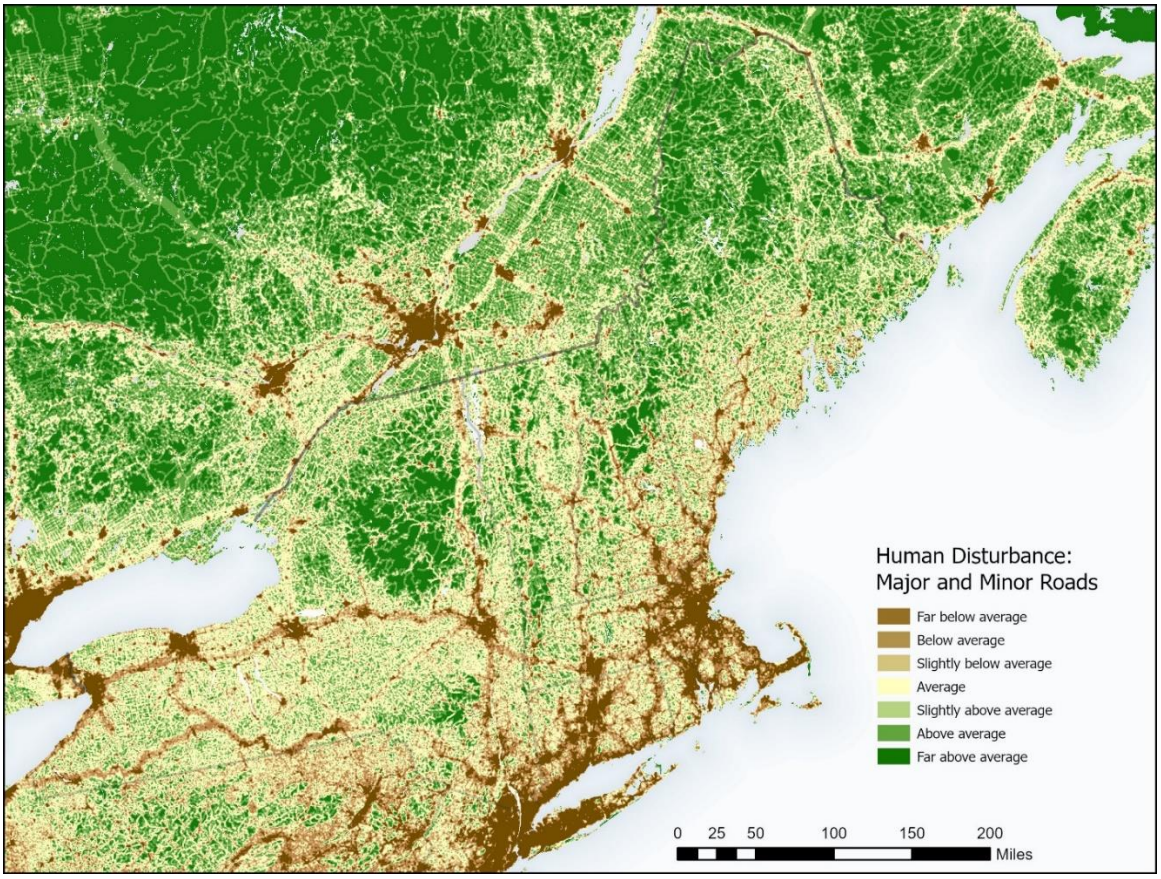

Figure 10: Road Density of Major and Minor Roads. The map shows the combination of the two density analyses using a 5 km search radius for major roads and 1 km radius for all other roads.

Validation of Human Disturbance

We focused on road density after preliminary tests indicated that density had greater explanatory power with respect to age and productivity by forest type than did block size or several other road related metrics. We did not validate the road dataset, but TIGER has evolved through three decades of digital transformations to become the authoritative national source for roads and boundaries.

Index of Geospatial Forest Condition

The index of geospatial forest condition can help us understand the extent to which forests retain their natural structure, composition, and ecological process. To calculate the index of geospatial forest condition, we combined the three forest condition attributes: forest turnover, forest height (stratified by habitat type), and human disturbance, assigning each attribute equal weight (Figure 11 and 12). A z-score, or standard normal score, measures how many standard deviations (sd) a particular data point is from the mean of the dataset. It is a way to standardize data on a common scale without changing the original distribution (Poldrack, 2023).. The forest height (stratified by habitat type) and road density were characterized using z-scores. The forest turnover attribute (percent turnover in 1000 acres) was transformed into a z-score. Then the three attributes were averaged to get one index of forest condition for each 30-meter grid cell in the Northern Forests. For mapping, average values were between -0.5 and 0.5 standard deviations (sd). Slightly above and below average were between 0.5 and 1 sds. Above (+) and Below (-) were between 1 and 2 sds. Far above (+) and below (-) were more than 2 sds.

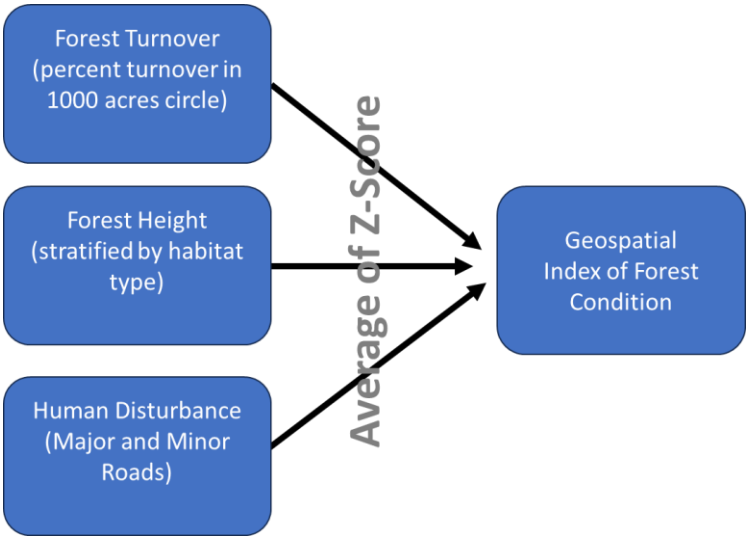

Figure 11: Creating the Geospatial Forest Condition Index. To create the geospatial forest condition index we equally weighted the three factors of forest turnover, forest height (stratified by habitat type), and human disturbance.

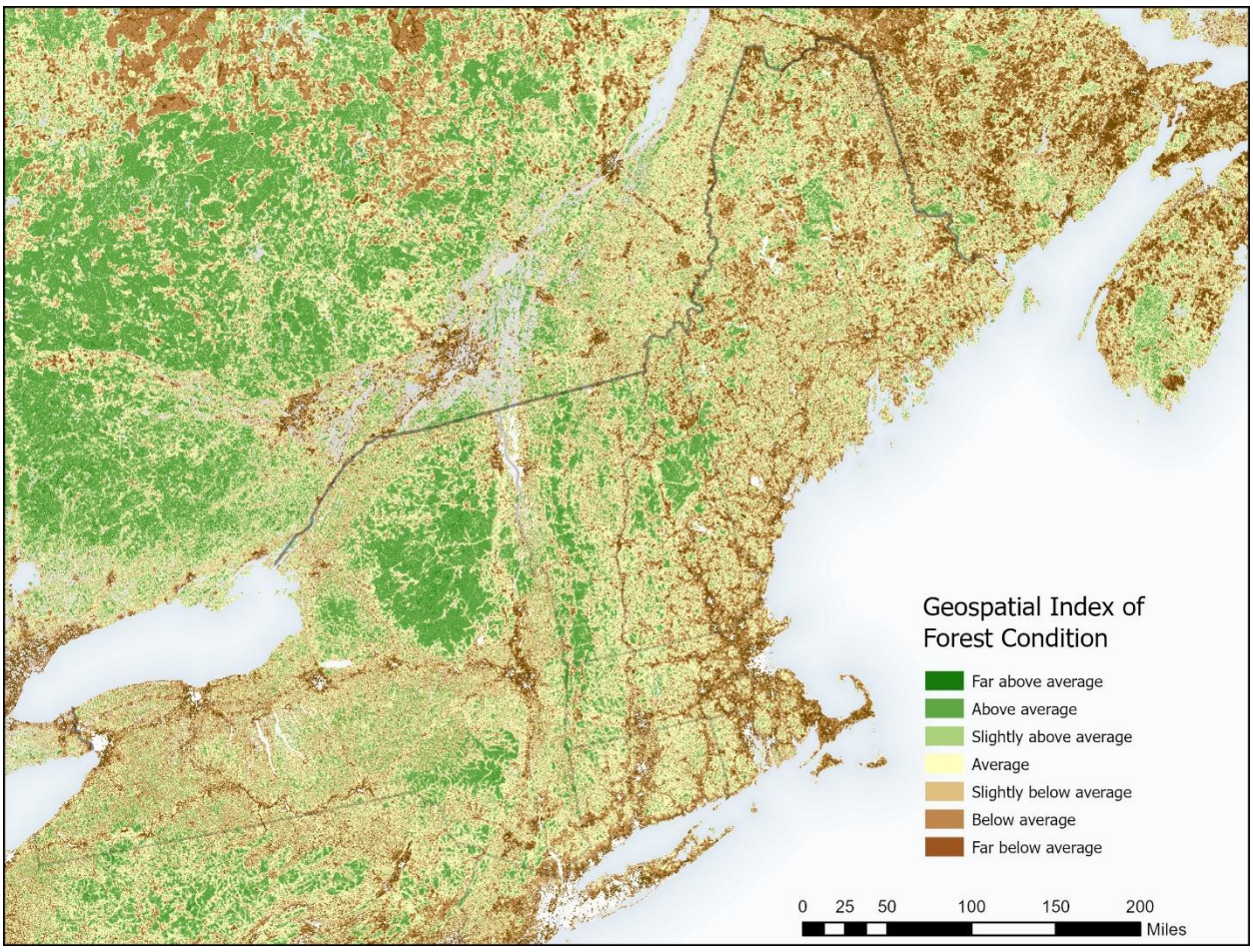

Figure 12: Geospatial Forest Condition Index. The map shows the final index of geospatial forest condition. In this index the three factors of forest turnover, forest height (stratified by habitat type, and human disturbance. These three factors are equally weighted. Validating the Geospatial Condition Index

Using data from The Nature Conservancy's Secured lands data, supplemented by Harvard Forest's wildlands data, we created a dataset of conserved lands likely to be in good condition (Olivero et al., 2023; Foster et al., 2023). This dataset included all lands permanently secured for nature and with natural processes (GAP 1) or management intended to sustain nature (GAP 2) by fee or easement with a public or private owner. These were augmented in a few non-permanent but long-term site in the Harvard Forest Wildland dataset. To account for tracts that were acquired immediately after harvest, the forest turnover on the tract had to be less than 5% between 2001 and 2023 to be included in the dataset. This resulted in a dataset depicting five million acres (4,389 records) of high condition forest (Figure 13).

To validate the geospatial forest condition metric, we created a dataset of 1000 random points that were in forests. Of that 1000 points, 71 fell in the potential high condition forests. The potential high condition forests had a significantly higher value (p value <.0001*) in the condition score (score = 1246) when compared to the other forests in the region (score = -76.44)

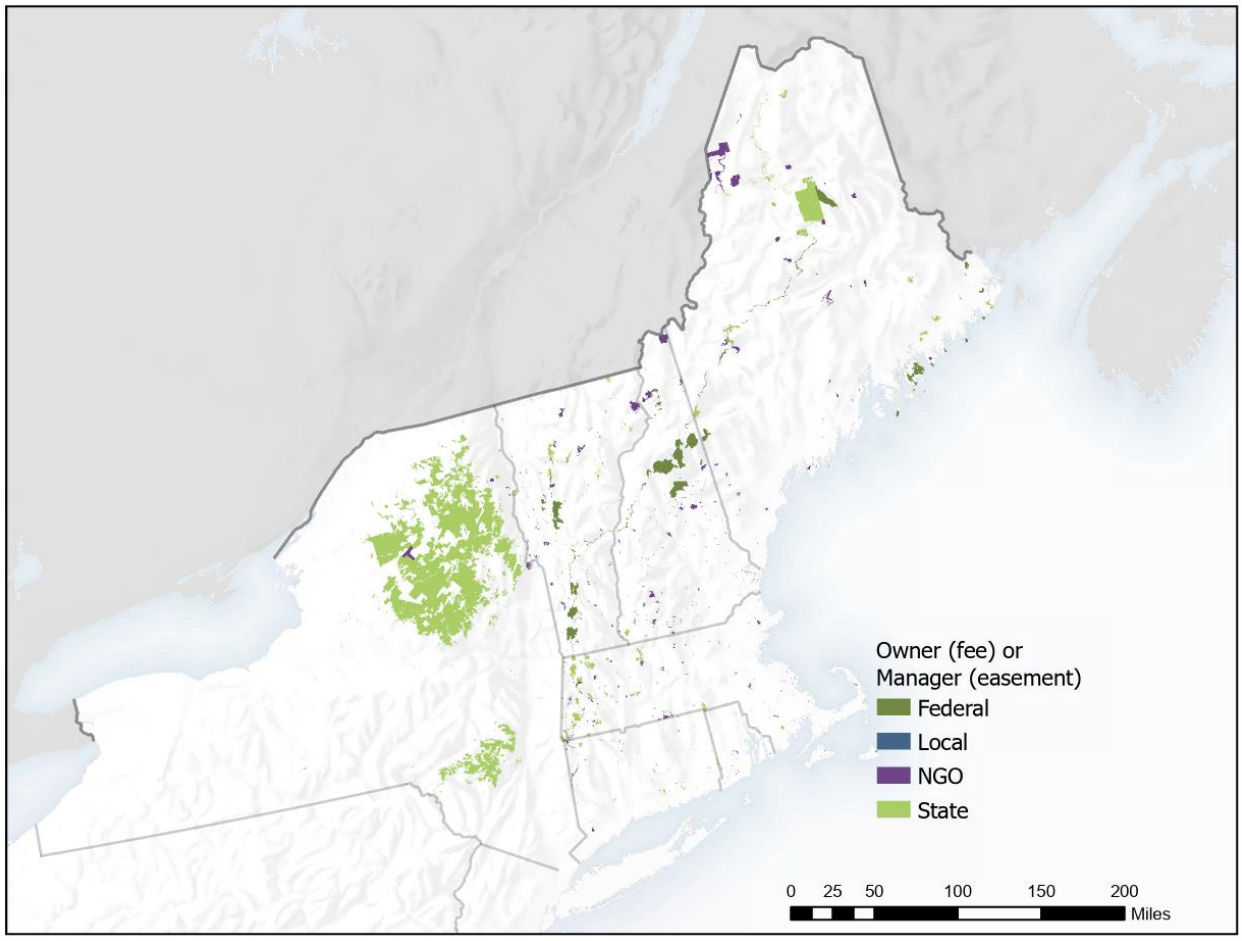

Figure 13: Potential high condition forests. This dataset was used to validate the geospatial forest condition index.

Forest Connectivity

Climate change is expected to alter seasonal temperature and precipitation patterns, and intensify disturbance cycles of fire, drought, and flood (Bolster et al., 2024). Rapid periods of climate change in the Quaternary, when the landscape was comprised of continuous natural cover, resulted in many changes to species distributions but few extinctions (Botkin et al., 2007). Now, pervasive fragmentation across the U.S. disrupts ecological processes and impedes the ability of many species to adapt to change, leading to depleted environments and lower biodiversity. Not surprisingly, the need to maintain connectivity has emerged as a point of agreement among scientists in how to help biodiversity adapt to climate change (Heller & Zavaleta, 2009; Krosby et al., 2010). In theory, maintaining a permeable landscape, when done in conjunction with protecting and restoring enough areas of high-quality resilient habitat, should facilitate the expected range shifts and community reorganization of species. Regional scale models suggest that the rate of natural migration for plants will not keep pace with the rate of climate change (Iverson et al., 1999, 2004; Iverson & McKenzie, 2013), highlighting the importance of local microclimate buffers and refugia where species can persist longer.

For this study, we defined connectivity as a measure of habitat permeability based on the physical features and arrangement forest condition factors presumed to be important for forest organisms to move and sustain ecological processes (modified from Hilty et al. (2019). We focused on continuous, wall-to-wall permeability rather than identifying specific linkages between pre identified places such as patches of good habitat, natural landscape blocks, or existing conservation lands (Barnett & Belote, 2021; Beier, 2012; Belote et al., 2022). Our emphasis on wall-to-wall connectivity reflects a goal of facilitating large-scale reorganization of species and habitats in response to climate change, which we suggest requires a comprehensive and continuous analysis: all organisms, in all directions, over many years. Thus, our aim was to create a model that reveals the implications of the landscape structure and condition with respect to the continuous flow of natural processes like dispersal, migration, and recruitment.

We developed two analytical models to assess different scales of continuous connectivity:

- *Local connectedness*, starts with a focal cell and estimates the connectivity of flows outward from the cell in all directions within a three-kilometer local neighborhood.
- *Regional flow*, examines broad east-west and north-south flow patterns across the entire region.

Both metrics rely on a “resistance grid” described below to model how the flow of movement can be facilitated, channeled, blocked, slowed, or redirected due to the spatial arrangement of land uses and their condition. Additionally, these analyses require high computational power, and make use of recent innovations in software and processing that allow for unprecedented speed and resolution (Hall et al., 2021; Hilty & Possingham, 2019; Theobald et al., 2022).

Resistance Values

The resistance surface is the foundation of the modeling process for both local connectedness and regional flow, whereby land areas are assigned resistance (or cost) values representing the hypothesized relationship between a cell’s ecological properties and the difficulty of animal movement across that cell. Electrical resistance measures how much a material impedes the flow of electrons whereas ecological resistance represents the ability, willingness, or likelihood that an organism will cross a particular environment. Impediments can include the physiological cost of moving through a unfamiliar or

dangerous environment, the reduction in survival for the organism moving through an exposed area, the lack of attractants or resources drawing the organism into the space, or a physical barrier to movement such as a closed canopy forest to a large soaring bird.

Creating a resistance grid is accomplished by parameterizing land cover variables along a continuum of how much they are expected to facilitate or impede natural species movement, where a low resistance denotes ease of movement, and a high resistance denotes restricted movement. We have found that it is not the absolute values assigned to the land cover that matter, but the relative values when viewed across all land cover types that determine the behavior of the flow as it is passed across the resistance surface.

Anthropogenic Resistance Values

The landcover data used to create the resistance grid was the 2021 NLCD in the US and 2020 Landcover dataset in Canada ((CCRS), 2020; Dewitz & USGS, 2023).To convert it to a resistance grid we applied weights to each land cover class where 10 = lowest resistance and 200 = highest resistance (Table 2 and Figure 14). These were based on the co-produced weights developed for the nation through a twelve-year study on climate resilience (Anderson et al., 2023) that included over 280 experts from federal agencies, state agencies. NGOs, universities, and Natural Heritage programs. The span allowed for a wide range of intermediate values.

We made several refinements and augmentations to the baseline landcover datasets to encompass roads and energy development as described below. Note that we did not include oil and gas production due to the small amount of land area devoted to it (Fractracker Alliance, 2024).

Landcover code (NLCD)	Landcover Description	Resistance Score	Source
21	Developed, Open Space	80	NLCD 2021
22	Developed, Low Intensity	80	NLCD 2021
23	Developed, Medium Intensity	90	NLCD 2021
24	Developed, High Intensity	200	NLCD 2021
31	Barren Land, non-natural	200	NLCD 2021
32	Barren Land, Natural	50	NLCD 2021
41	Deciduous Forest	10	NLCD 2021
42	Evergreen Forest	10	NLCD 2021
43	Mixed Forest	10	NLCD 2021
52	Shrub/Scrub	50	NLCD 2021
71	Grassland/Herbaceous	50	NLCD 2021
81	Hay/Pasture	60	NLCD 2021
82	Cultivated Crops	70	NLCD 2021
90	Woody Wetlands	10	NLCD 2021
95	Emergent Herbaceous Wetlands	50	NLCD 2021

Table 2. Resistance weights. This table show the resistance value applied to each landcover class to convert the landcover data into the foundation of a resistance grid.

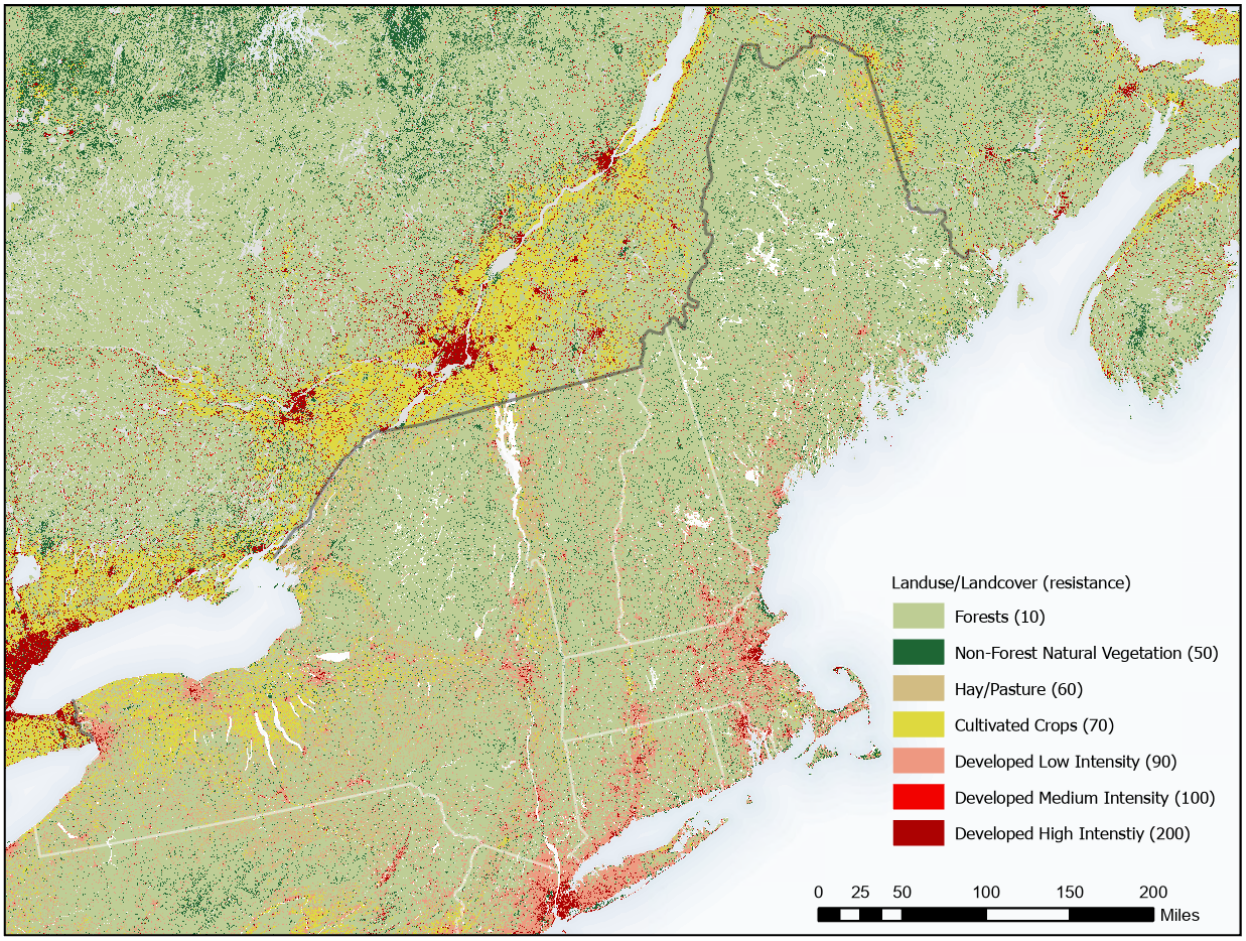

Figure 14. Landuse and Landcover with resistance values.

Wind Turbines

Although wind power is one of the cleanest and most sustainable energy sources, there are local impacts that may affect the connectedness of the area immediately surrounding a turbine. The landcover at the base of the wind turbine is permanently disturbed, and a larger area is disturbed during construction. There are also impacts from the roads connecting the turbines. Research is ongoing on the effect of turbines on wildlife. The impact on birds and bats is the most well studied and the area of impact varies depending on the species.

To map the distribution of wind turbines and farms we used the United States Wind Turbine Database which is a joint project funded by U.S. Department of Energy, Wind Energy Technologies Office, via the Lawrence Berkeley National Laboratory, Electricity Markets and Policy Group, the U.S. Geological Survey's Energy Resources Program, and the American Wind Energy Association (Hoen et al., 2022). This is a continuously updated GIS dataset of land-based and offshore wind turbines in the United States. For our study area we found 1,910 mapped wind turbines are in Maine, New Hampshire, Vermont, and New York with an additional 2,034 turbines in the extended area (Hoen et al., 2022).

To represent wind energy development in the resistance grid dataset, we summarized the density of turbine using a 1-mile kernel radius and added it to the base resistance score (Table 3). For example, an area withs 4-8 turbines per square mile (resistance = 6) and natural cover (resistance = 10) received

Wind Energy Turbine Density	Added Resistance Weight
0 - 1 turbines per square mile	0
1 – 2 turbines per square mile	2
2 – 4 turbines per square mile	4
4 -8 turbines per square mile	6
Greater than 8 turbines per square mile	8

Table 3: Resistance weights for wind turbine density.

resistance value of 16. An agricultural area that has 4-8 turbines per square mile received a resistance score of 70 (agriculture) plus 6 (turbines) = 76.

Solar Energy

Solar Energy is another essential source of clean energy, but the actual land where a solar field is sited, may create negative impacts on connectivity. The area is typically fenced off to prevent vandalism and damage from larger animals, and most of the land surface is covered with solar energy panels. No single map of solar energy polygons currently exists, but the EPA eGRID renewable energy data has latitude/longitude for all energy facilities across the country (U.S. EPA, 2024). We filtered this dataset for just solar energy and hand digitized the spatial extent of each solar energy facility using National Agriculture Imagery Program (NAIP) imagery (USDA Farm Services Agency, 2019). To account for the decrease in connectivity on the site, we gave solar energy sites a resistance score of 200 equivalent to high-intensity developed land.

Barrens and mines

In the land cover datasets, the category “barrens” often mixes developed lands such as oil and gas wellheads with natural barrens such as riparian areas, mudflats, and sandy bare soil. In a previous project we revised the NLCD (2011) landcover using a variable search radius around each barren to classify them as developed or natural. All barrens classified as developed in 2011 were similarly classified as developed in 2021. Also, to confirm our classification, we visually inspected all barrens larger than 100 acres using satellite imagery and manually assigned them to one category or the other.

Natural barrens were assigned a resistance score of “50,” the same as natural non-forested cover. Natural barrens are often beaches, lakeshores, and rock alpine environments. Developed barrens and surface mines were assigned a resistance score of “200” to reflect their modified nature.

Roads

To account for roads and road impacts we used the augmented TIGER road datasets described above in conjunction with the impervious surface description raster of the NLCD 2021 (Dewitz & USGS, 2023). The road dataset groups roads into three classes: primary, secondary, and tertiary. For Canada we classified the OpenStreetMap roads into the same categories Primary (fclass = primary, motorway, trunk), Secondary (fclass = secondary), and Tertiary (fclass = tertiary, unclassified, residential). Primary and Secondary roads were assigned a resistance score of a 200 (Geofabrik, 2022b). Tertiary roads were assigned a resistance score of a 100. We did not include dirt roads in the resistance grid, but they were used in the road specific analysis.

Integrating Geospatial Forest Condition into the Resistance Grid

This forest condition project is unique because it incorporates forest condition into the resistance grid. Most connectivity model resistance grids are based off a landuse/landcover grid, but resistance grids can also include hydrology, slope, snow cover, etc. (Aylward et al., 2020; Balestrieri et al., 2019; Schoen et al., 2022; Zeller et al., 2012). By modifying the resistance grid to include forest condition we can model the impact of forest condition on connectivity and identify places where changes in condition would have the largest impact on connectivity.

For the resistance grid the scores ranged from 10 to 200 with the highest resistance (200) set as developed, and the rest of the anthropogenic values parameterized as described above with the lowest resistance for a non-forest landuse being non-forest natural lands such as grasslands with a resistance score of 50. Forested lands received resistance scores between 49 (worst condition) and 10 (best condition). We used the three forest condition attributes from the forest index, but combined them with the parameterization required for resistance grids in connectivity models (Figure 15).

Forest Turnover: For forest turnover, we parameterized the resistance based off of the years since forest loss. Both the local connectedness model and regional flow models are wall-to-wall continuous models that take a neighborhood approach, therefore using the loss year on the cell (as opposed to the neighborhood value) was most appropriate. For forest loss values, we spread the values of years since loss (1 -22 years) to the resistance values between 30 and 50, with 22 years given a resistance score of a 30 and 1 year since loss given a score of a 50.

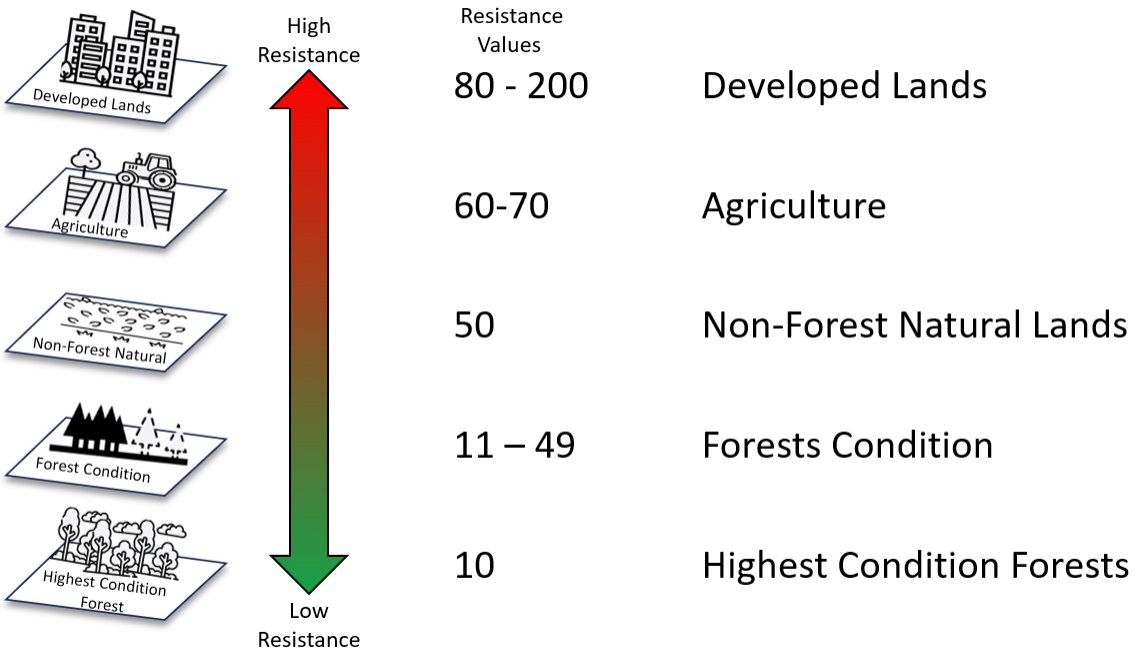

Figure 15: Development of the Resistance grid.

Forest Height: For the resistance grid for connectivity, forests that have remained stable over the last 22 years have higher condition than forest that have experienced turnover. The forest height (stratified by habitat type) was given a resistance score from 10 to 30. We used the Z-Score values and linearly transformed the values to the 10 to 30 scale with 10 having the tallest forests by habitat type and 30 having the shortest forests by type.

Human Disturbance: All forested areas, both those that have experience turnover and stable forests, experience impacts to their forest condition due to human activities. For the human disturbance factor, we used the Z-Score values for human disturbance from the condition index and linearly transformed the values on forested cells to a 10 to 50 scale with 10 least amount of human disturbance and 50 having the most amount of human disturbance.

Combining Condition Factors: To combine the three condition attributes, we average the combined forest turnover and forest height value with the human disturbance layer. Human disturbance is part of the anthropogenic resistance values, and we wanted to highlight the conditions based on forest attributes, so we weighted the forest attributes of forest turnover and height 4 times as much as the human modification based on testing of a variety of weighting schemes. This resulted in a resistance grid that combined anthropogenic landuse and forest condition (Figure 16).

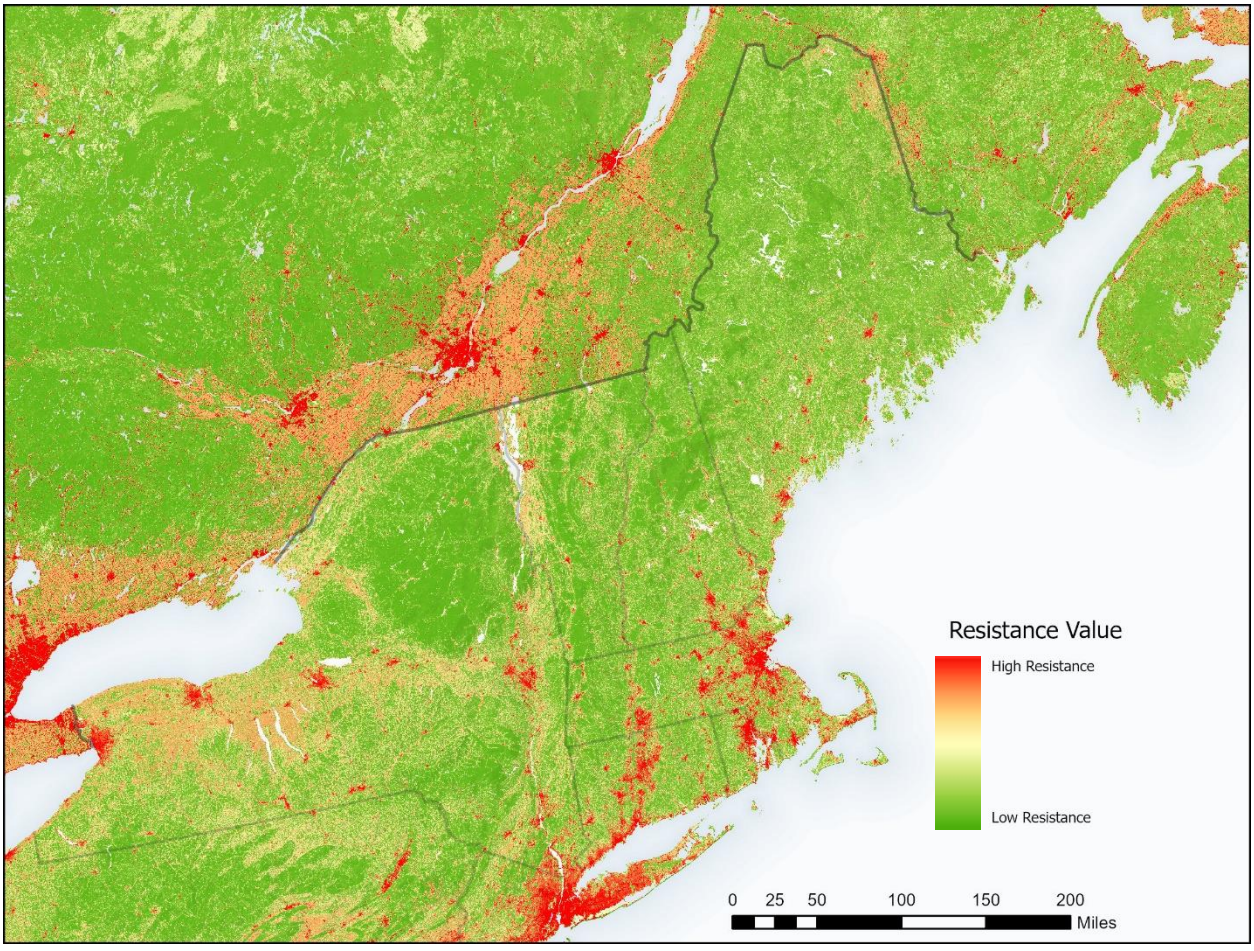

Figure 16. The combined resistance grid for anthropogenic landuse and geospatial forest condition.

Local Connectedness

Local connectedness estimates the permeability of the landscape directly surrounding a focal cell if movements were to flow outward in all directions from its center point(Compton et al., 2007; McGarigal et al., 2018). Because of its local focus, this metric estimates how easily species can access nearby microclimates or other resources given the arrangement of roads, industrial agriculture, development, and other factors that form barriers or increase risk. In the model, the permeability of two adjacent cells increases with the similarity of those cells with respect to their land cover. If adjacent landscape elements are identical (e.g., forest - forest), then there is no disruption in flow. A contrasting element (e.g., forest - developed) creates resistance and the connection is presumed to be less permeable. The degree to which a cell alters the flow arriving from an adjacent cell is its "resistance" and the corresponding land use is assigned a resistance weight based on its expected resistance to movement derived from the sharpness of contrast in structure, surface texture, or exposure.

The method used to map local connectedness for the region was resistant kernel analysis (Compton et al., 2007). To calculate this metric, we used the condition based resistance grid described above aggregated to 90 meters (for computational efficiency). As physical landscapes are naturally composed of an interacting mosaic of different ecosystems, our goal was to locate areas where these arrays occur in such a way as to maintain their natural relationships and the connections between all types of flows, both material processes and species movements, not to maximize permeability for a single species (Ferrari & Ferrarini, 2008; Forman & Godron, 1986; Hunter et al., 2021). The result of the analysis is a continuous grid of 90-m cells where each cell was scored with a local connectivity value from 0 (least connected) to 100 (most connected) based on a distance weighted analysis of the resistance in a 3-km radius around each cell. For display purposes, we Z-scored these values to put them on a standard normal score (Figure 17).

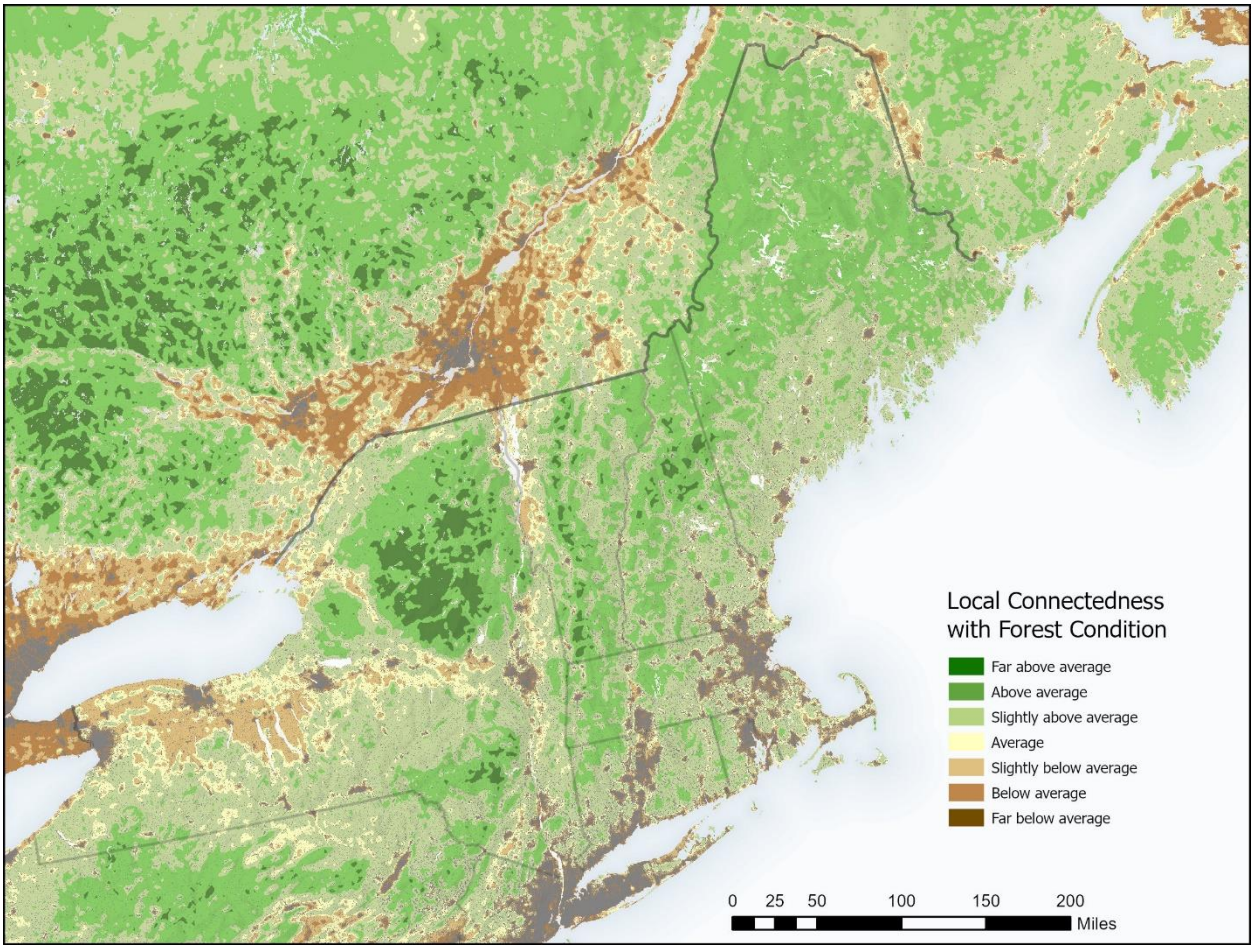

Figure 17. Local Connectedness with Geospatial Forest Condition.

While knowing the local connectedness value taking into account the current condition of forests is useful, knowing where improvements to forest condition can have the greatest benefit can help strategically plan forest management, conservation, and restoration. To accomplish this, we measured the difference between local connectedness with current forest condition and local connectedness with forests at their best possible condition (resistance of all forests = 10) to identify areas where improving the condition of forests would have the greatest impact on local connectedness (Figure 18). For this metric keep in mind that areas currently in good condition already facilitate local connectedness, so there is little room for improvement in the local connectedness scores. Conversely, in developed or agricultural areas, the higher intensity landuses are largely driving the local connectedness scores, so improving forest connectivity in these areas will also not have a large impact on the local connectedness scores.

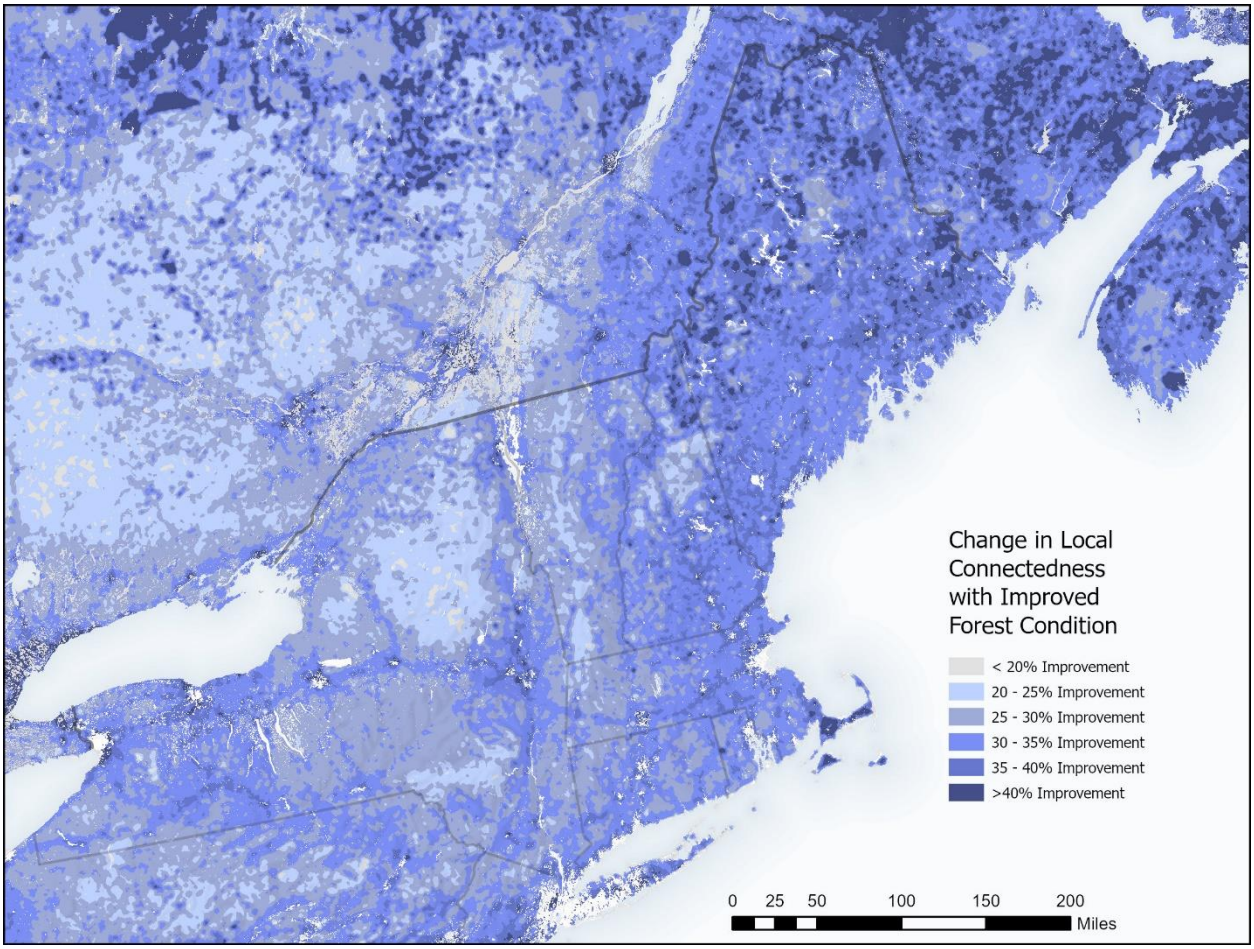

Figure 18. Change in Local Connectedness with Improved Geospatial Forest Condition.

Regional Flow

To quantify larger scale directional changes in connectivity resulting from the cumulative effects of land use, land management, and other sources of resistance, we used a wall-to-wall Circuitscape model (Pelletier et al., 2014). Circuitscape estimates the density of "current flow" across a resistance surface as a proxy for natural movements. The resistance surface is a grid, or set of grids, comprised of landscape features, with each feature weighted by its relative resistance to movement (Dickson et al., 2019; Shah & McRae, 2008). When the Circuitscape model is run, each cell receives a quantitative score reflecting the amount of current channeled through the cell as a function of its location, context, resistance, and direction of flow.

To obtain a multi-directional and wall-to-wall coverage of the region we ran the model using the resistance grid described above, aggregated to 90 meters for computational efficiency. We divided the resistance grid into landscape tiles where one whole side of the tile was assigned to be "source" and the opposite side to be "ground." Next, "current" was injected along the entire source side and allowed to flow across the landscape resistance surface towards the ground side. As the current flows it reveals the various flow pathways and highlights where flow gets blocked or concentrated. Because current seeks the path of least resistance from the source cells to any grid cell on the ground side, a run with the westside as source and the eastside as ground will not produce the same current map as a run with the eastside as source and westside as ground. Runs were thus repeated in each of four directions: east to

west, west to east, north to south, south to north, and summed across all directions. Lastly, we clipped out the central quarter of each tile and joined it to the central regions of all the other tiles. This last step was done because testing had shown that the central quarter gave stable, repeatable, and consistent results regardless of the size of the calculation area. In contrast, the outer margins of the tile had considerable noise in the results created by the tile's exact boundaries. All calculations were performed using the latest version of Circuitscape (5.0) implemented in Julia with a cell size of 90 meters.

We developed a systematic and repeatable processing method to run the analysis and then used Python and Julia scripting to automate the process. First, the study area was divided into 16 tiles (calculation areas) comprised of 7000 cells by 7000 cells. Each tile was intersected with the resistance map and the analysis was run as described above. All tiles with land cover information were included except for those that were 100% water (ocean) which were given a neutral grid of values (Clark et al. under review 2025).

The wall-to-wall results reveal spatial patterns in current flow that reflect the relative intensity of the various human-modifications to the landscape and how they are configured to facilitate or inhibit flow (Figure 19). Analyzing and classifying the flow allows users to identify where population movements and potential range shifts may become concentrated or where they are widely dispersed. It is possible to quantify the importance of an area by measuring how much flow passes through it and how concentrated that flow is. We created a categorical classification of flow pattern to capture this information in the final wall-to-wall connectivity and climate flow map, by applying the following method. First, we calculated the amount and the variation of flow in every local neighborhood (404.686 hectare, 1000 acres) around every cell (the size of the neighborhood was determined by testing a variety of distances and picking the one that best captured flow pattern and still retained local detail and it matches the radius used for landscape diversity in the Resilient and Connected Network project). Next, within each neighborhood we calculated the mean amount of flow, and the variation in flow as indicated by the standard deviation. Areas that had high flow and a high standard deviation were considered "concentrated" because they not only channel a large amount of flow but are different from their surrounding cells. Areas that had above-average flow and low standard deviation were considered "diffuse" because they move a lot of flow but are similar to their neighboring cells. We divided the mean and standard deviation into 7 quantile classes by area and analyzed the combinations to classify the wall-to-wall continuous grid. (Figures 20 and 21). The three prevalent flow types found here each suggest a different conservation strategy:

- Diffuse flow: areas that are extremely intact and consequently facilitate high levels of dispersed flow that spreads out to follow many different and alternative pathways. A conservation aim might be to keep these areas intact and in good condition to prevent the flow from becoming concentrated. This might be achievable through forest management or broad-scale conservation easements.
- Concentrated flow: areas where large quantities of flow are concentrated through a narrow area. Because of their importance in maintaining flow across a larger network, these pinch points are good candidates for land conservation.
- Blocked/Low flow: areas where little flow gets through and is consequently deflected around these features. Some of these might be important restoration areas, where restoring forest cover or altering road infrastructure might reestablish a historic connection.

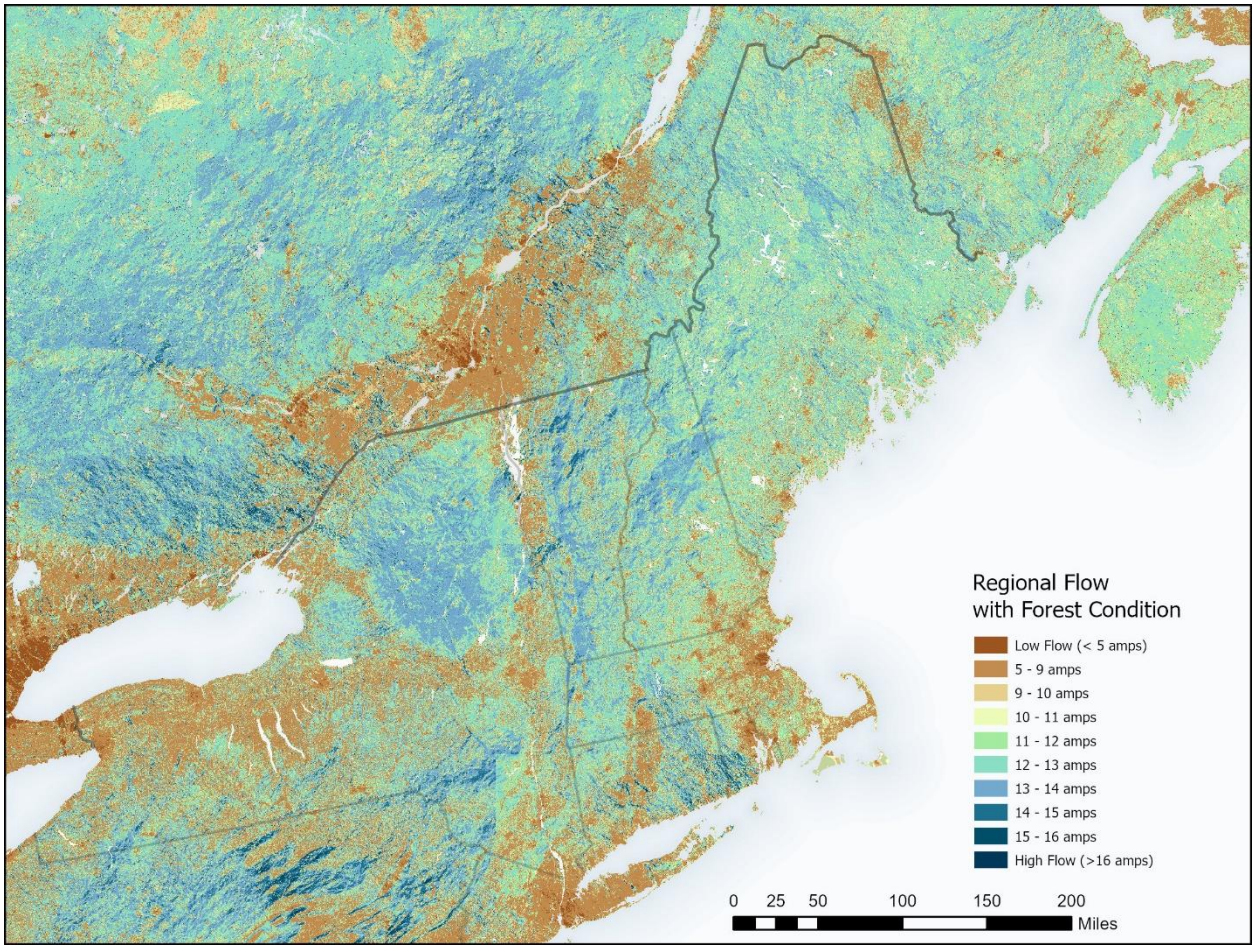

Figure 19: Regional Flow with Geospatial Forest Condition. Brown indicates areas with low permeability. Light blue indicates areas of moderate flow; often highly natural settings were species movements are diffuse. Dark blue indicates areas of concentrated flow where movements will accumulate or be channeled.

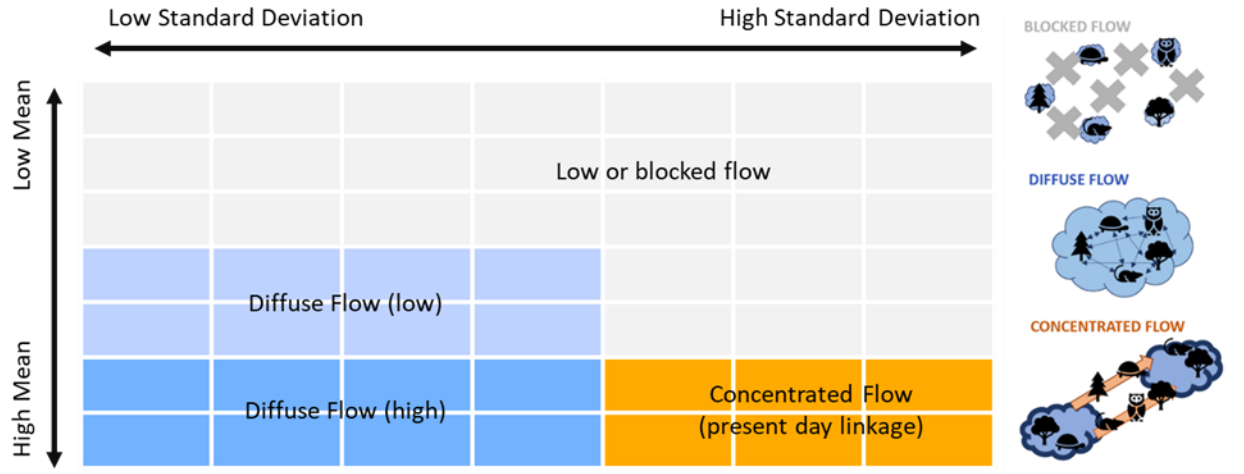

Figure 20: Description of the classification of flow into categories.

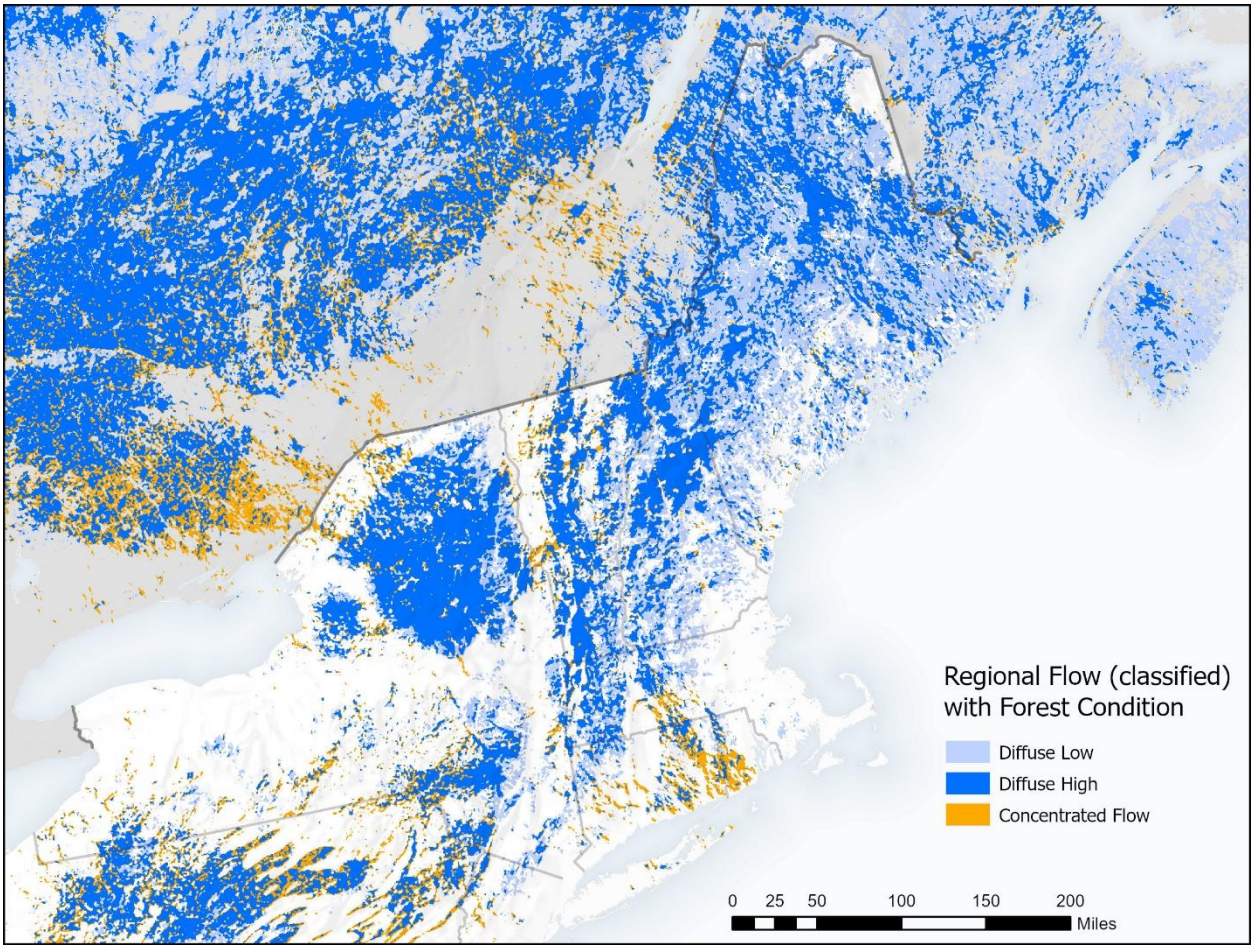

Figure 21: Classified regional flow with geospatial forest condition resistance. White areas indicate areas with low permeability where movement is blocked. Blue indicates areas of moderate flow; often highly natural forests in good condition where species movements are diffuse. Orange indicates areas of concentrated flow where movements will accumulate or be channeled through a pinch point.

Similar to local connectivity, knowing the regional flow taking into account the current geospatial condition of forests is useful, but for conservation and restoration knowing where improvements to forest condition can have the greatest benefit can help strategic conservation and management. We measured the difference between regional flow with the current forest condition and regional flow with the forests in the highest condition (resistance of all forests = 10) to identify areas where improving the condition of forests would have the greatest impact on regional flow (Figure 22). It is important to note that this metric measures the change in flow if the geospatial forest condition of **ALL** forests were improved, not the flow that would be improved with individual project or parcel improvement of condition. Next, we measured the change in the classes of flow with improved condition. With improved condition, we see additional areas of diffuse and concentrated flow, increases from low diffuse flow to high diffuse flow, and changes from concentrated flow to diffuse flow (Figure 23).

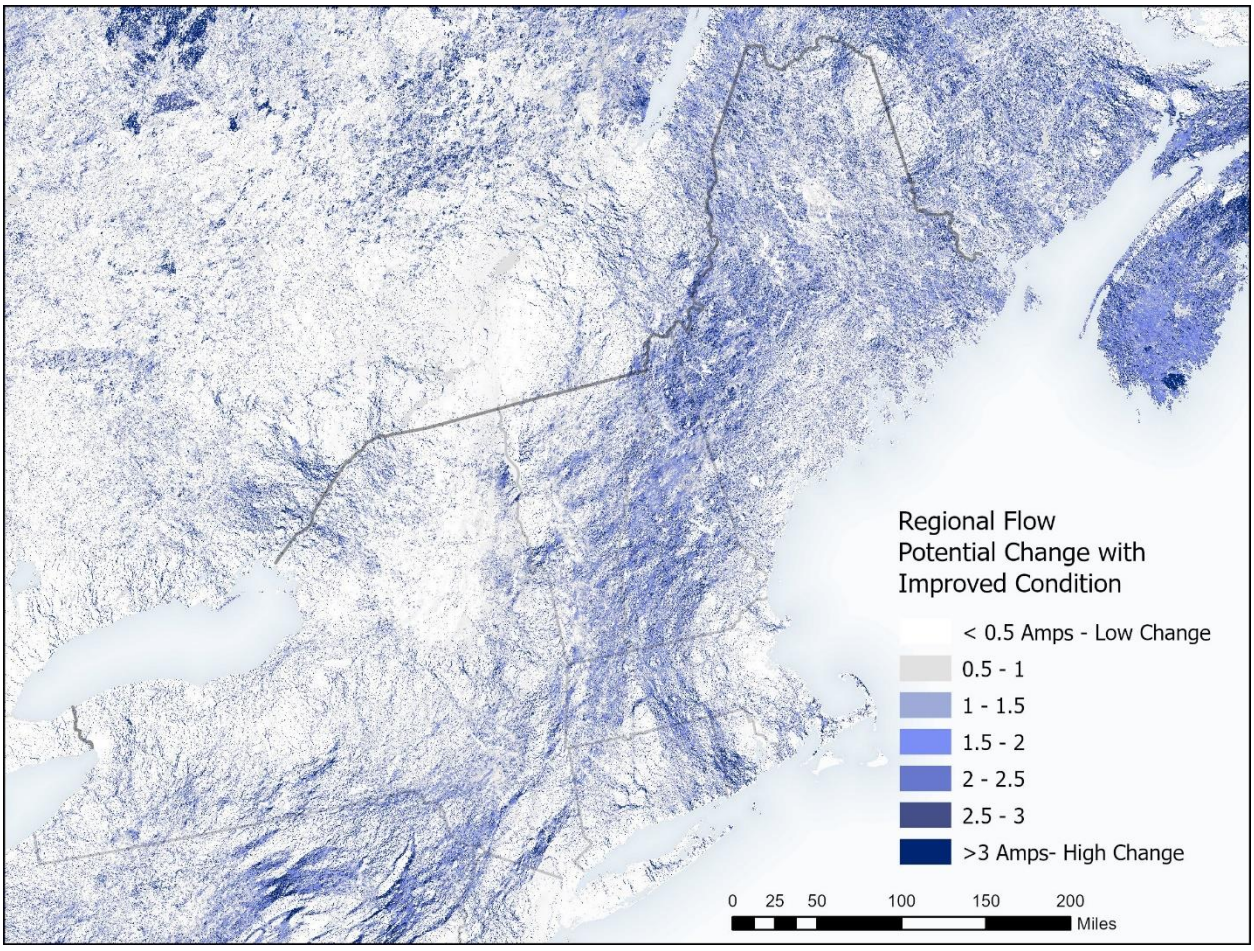

Figure 22: Regional Flow Potential Change with Improved Condition.

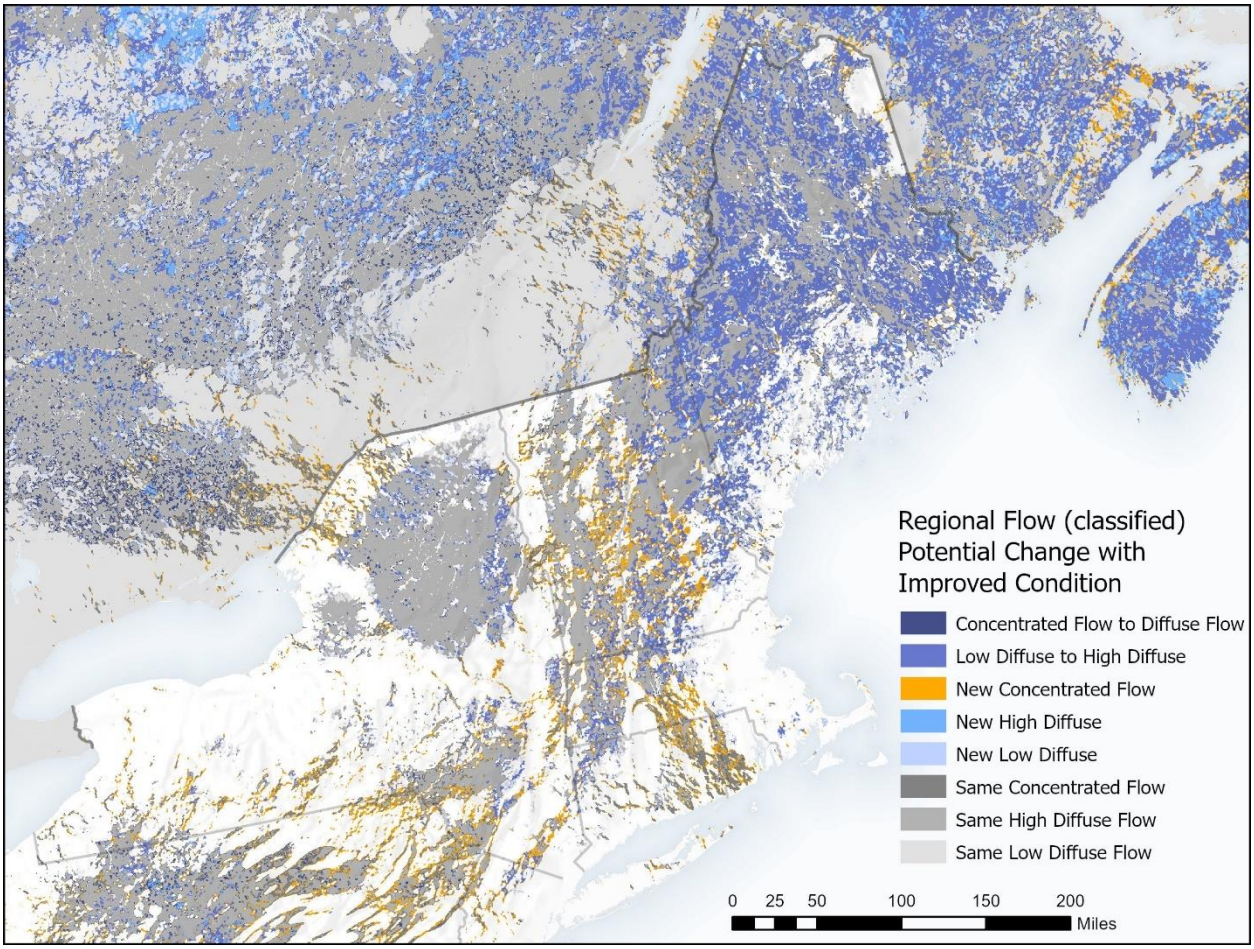

Figure 23: Regional Flow Classified Potential Change with Improved Condition.

Connectivity, Climate and Condition

Climate Flow

The effect of climate change on a species is complex and intertwined with patterns of soils, vegetation and hydrologic flow paths (Groffman et al., 2012). The capacity for a species to respond to climate change is dependent on species population traits and the rate, magnitude, and direction of climate change (Dawson et al., 2011).

Species Responses to Climate Change:

A variety of ecological factors may create variation in individual species' response to climate: competitive release, habitat modification, or changes in amounts and patterns of precipitation, snow cover duration, water balance, or seasonality (Groffman et al. 2012). A coherent climate footprint does not require that all species show the same climate change response (Parmesan & Yohe, 2003a). Recognizing that not all species respond to climate change the same way, there are still some general trends that have been well-documented in individual studies and meta-analyses.

Poleward: Poleward movement is the best documented species response to climate change. In a comprehensive analysis of tree species in the eastern US, it was shown that 67% of species are moving northward. Poleward movement due to climate change has also been identified in North American bird

species (Hitch & Leberg, 2007; Zuckerberg et al., 2009), lichens (van Herk et al., 2002), and butterflies (Parmesan et al., 1999). The Arctic and Antarctic are experiencing some of the fastest warming rates; several early studies have shown poleward range expansions (Hersteinsson & MacDonald, 1992; Smith, 1994; Sturm et al., 2001). Presumably these species are tracking warming temperature gradients.

Upslope: Species may also track warming temperature gradients by moving upslope. In the French highlands, a study of 424 forest plant species found that cold-adapted species are declining in lowlands at the warm margin of their ranges. In contrast, warm-demanding species are expanding into highlands that correspond to the cold margin of their range (Kuhn & Gégout, 2019). Researchers in Yosemite National Park found substantial upslope movements for over half of the species monitored (Moritz et al., 2008). Near the equator, studies have found ample evidence of upslope movement suggesting that most climate relief in the tropics comes from elevational gradients, not poleward movements (Pounds et al., 1999).

Poleward and Upslope: Meta-analysis revealed that across the globe many species are moving both poleward and towards higher elevation at a median rate of 11 meters per decade and upslope at 16.9 km per decade (Chen et al., 2011). These responses are consistent across taxonomic groups with more variation found among groups rather than between groups (Chen et al., 2011). A high elevation meta-analysis of birds, butterflies, and alpine herbs found that climatic shifts were on average 6.1 km poleward or 6.1 meters upward per decade (Parmesan & Yohe, 2003).

Moisture: Where climate change has resulted in drought or drying, there is evidence of shifts toward moisture with movement trending downslope towards valley bottoms and riparian areas that offer cool, moist microclimates relative to surrounding areas (Beier, 2012; Dobrowski, 2011,. Olson et al., 2007). In a study of 64 plant species in California, Crimmins et al. found that climate change has resulted in a significant downward shift in species distribution (Crimmins et al., 2011). In a study of eastern US trees, (Fei et al., 2017) found 73 % of species were adjusting their ranges to track moisture. For plants, moisture may be more important than temperature but population responses to moisture and precipitation changes is the least predictable and the least studied effect of climate change.

Flat areas with little topographic relief are especially vulnerable to climate change. The distance between an area's current temperature and the same temperature in a future climate change scenario, its climate velocity, is high in low relief areas and may lead to vulnerability (Dobrowski & Parks, 2016; Loarie et al., 2009).

Mapping Climate Connectivity

A permeable landscape and a connected network of sites will allow many species to move and rearrange in their individual ways. In the past, during periods of rapid climate change, the ability for species to rearrange is a crucial reason scientists think there were relatively few extinctions (Botkin et al., 2007).

The connectivity and climate flow model developed here is based on environmental gradients of upslope, poleward, and moisture movement, combined with anthropogenic resistance augmented to include forest condition. The model uses wall-to-wall Circuitscape combined with a sophisticated resistance grid that goes beyond landcover to include the condition and quality of forest features as well as topographic and elevational resistance and northward directional flow. Because we are modeling geophysical climate gradients based on the mean or modal species response we avoid the uncertainties of individual species responses to climate change.

This dataset marks an advancement in the scale of the analysis and in the use of a resistance grid that integrates ecological condition and quality along with topographic and directional gradients as factors that facilitate or direct species movement. This allows for a defined level of confidence in a climate change signal on a regional scale (Parmesan & Yohe, 2003b).

To develop a map of climate flow, we recast the three main ways species ranges are shifting in response to climate (upslope, downslope, and poleward) as changes in resistances (Anderson et al., 2018).

Upslope Flow

The upslope resistance model highlighted areas with high potential for upslope range shifts both locally and across the region. To model upslope movement we created a 30-m continuous landform model that classified cells based on relative land position and slope into discrete landscape features (i.e. steep slopes, upper flats, wet flats) (Anderson 1999, Anderson et al. 2012). We converted this to a resistance grid using land position and slope. First, we isolated the relative land position value and assigned increased resistance to moving downslope and decreased resistance to moving upslope. Next, we modified the resistance score using the cell's slope value, to reflect the relative degree of effort versus gain in temperature differences (Table 26). For example, moving upward along a gentle slope is easy but provides little gain in lower temperature (moderate resistance), moving upward along a moderate slope provides larger gains in temperature differences for moderate effort (low resistance), moving upward along a steep slope is too difficult for most species despite the rapid change to lower temperatures. We averaged the land position and slope values into one resistance score. Finally, the resistance on cooler aspects (north facing sideslopes and coves) was reduced slightly (0.5 pts) with respect to warmer aspects. Although mountainous areas may produce the largest amount of pure elevation change, species also experience temperature relief from slopes relative to their local landscape (e.g., a two degree slope in a flat landscape may provide more relief to nearby species than a five degree slope in an already mountainous landscape). To ensure that the upslope resistance grid was scaled to both local temperature relief and larger regional temperature relief we calculated both a regional resistance score and a local neighborhood resistance score around each cell and then averaged them. For regional relief we calculated the absolute amount of upslope resistance in a three km focal area around each cell and converted it to a Z-score using the mean and standard deviation for each ecoregion This distance matches the distance used to measure scale movement in Anderson et al.'s climate resilience work (M. G. Anderson et al., 2014, 2019). For local relief, we used the same focal statistic algorithm to calculate the mean and standard deviations of upslope resistance for a three km local radius around each cell and converted the flow to a Z score using only these local means and deviations. The distributions of the regional and neighborhood z-score datasets were very different such that the local neighborhood resistance score overwhelmed the regional score. Therefore when we averaged them, we gave twice the weight to the regional resistance grid. The results provided a single upslope resistance grid that was a weighted combination of regional and local resistance.

To incorporate anthropogenic features into the resistance grid, we combined the upslope resistance grid with the anthropogenic resistance grid weighting the scores so that the final resistance score of each cell was 50% from the upslope resistance value and 50% from the anthropogenic resistance value.

Table 4: Resistance scores applied to landform model. Land position ranks (LP rank) were ordered so they decrease towards higher land positions. Slope rank were ordered so that they increase at the extremes of no slope (no temperature gain) and steep slopes (too difficult to transverse) and are lowest at moderate values.

Landform	Slope	Position	Land Position rank	Slope rank	Sum	Weight
Steep slope	4 high	any	NA	9	18	9
Cliff	5 highest	any	NA	10	20	10
Flat summit	1 flat	highest	1	7	8	4
Slope crest	3 moderate	highest	1	1	2	1
Hilltop flat	1flat	high	4	7	11	5.5
Gentle slope	2 gentle	high	4	4	8	4
NE sideslope	3 moderate	high	4	1	5	2
SW sideslope	3 moderate	high	4	1	5	2.5
Dry flat	1 flat	low	7	7	14	7
Wet flat	1 flat	low	7	7	14	7
Lower side	3 moderate	low	7	1	8	4
Slopebottom flat	1 flat	lowest	10	7	17	8.5
Slopebottom	2 gentle	lowest	10	4	14	7
North cove	3 mod	lowest	10	1	11	5
South cove	3 mod	lowest	10	1	11	5.5

Although mountainous areas may produce the largest amount of pure elevation change, species also experience temperature relief from slopes relative to their local landscape (e.g., a two degree slope in a flat landscape may provide more relief to nearby species than a five degree slope in an already mountainous landscape). To ensure that the upslope resistance grid was scaled to both local temperature relief and larger regional temperature relief we calculated both a regional resistance score and a local neighborhood resistance score around each cell and then averaged them. For regional relief we calculated the absolute amount of upslope resistance in a three km focal area around each cell and converted it to a Z-score using the mean and standard deviation for each ecoregion. We linearly rescaled the z-scores from a 1 to 10 scale to create a resistance grid and then ran wall-to-wall circuitscape with only the upslope flow.

Moisture/Downslope Flow

To model flow towards moist areas, we first identified areas that were down-gradient and lower in elevation than the surrounding landscape. This created a more detailed map of downslope flow than using landforms alone. We created a 30-m dataset that assigned a relative elevation value to every cell by comparing its elevation from the digital elevation model to its neighbors within a three km neighborhood (the same radius used calculate upslope local flow and to calculate local connectedness in the Resilient and Connected Network study) (M. G. Anderson et al., 2023; U.S. Geological Survey, 2019). In a similar method to the upslope flow, we used focal statistics to calculate the mean and standard deviations of the elevations within a 3 km radius, and then calculated a Z-score for each cell based on the neighborhood mean and standard deviation. Values below the mean were lower than their neighborhood and provide more downslope temperature relief, and we assigned them less resistance.

Values higher than the mean were higher in elevation than their neighborhood and had less downslope climate relief and were assigned higher resistance values. To give additional benefit to flow in moist areas, we integrated the landform model (Anderson 1999) into the resistance grid and further lowered the Z score within moister landforms. Areas of coves, pluvial moist flats, and wet flats were extracted from the landform dataset and their Z-Score for the resistance grid was lowered. Coves were lowered to one quarter (-0.25) standard deviations below average, pluvial landforms were lowered to one half (-0.5) standard deviations below average, and wetlands were lowered to (-1.0) standard deviations below average if the elevation-based Z score was not already less than these scores. This lowered the resistance slightly in moist and wet areas allowing current to flow more easily. We linearly rescaled the z-scores from a 1 to 10 scale. We linearly rescaled the z-scores from a 1 to 10 scale to create a resistance grid and then ran wall-to-wall circuitscape with only the downslope flow.

Poleward Climate Flow

We added latitudinal direction into the climate flow model to simulate long-term climate relief for populations that expand or shift northward. We did this by weighting the north-south runs twice as much as the east west runs when combining the four directional runs we used to develop the regional flow model (i.e., north to south, south to north, east to west, and west to east, see previous section for details).

Integration of Anthropogenic and Climate Flow

For our final geospatial forest condition map with climate flow, we weighted the forest condition based regional flow model with the upslope, moisture/downslope, and poleward models to simulate how species populations could flow through the natural landscape finding climate refuge both by moving up or down slopes and mostly in a poleward direction. The goal was to approximate a species population expanding locally then poleward as allowed by the forest condition and anthropogenic resistance within its neighborhood. When combining the factors, a challenge was how to weight the influence of each factor in a way that most closely approximates the real world. We wanted to keep the emphasis on the areas that are important for the forest condition-based anthropogenic flow, while boosting slightly the areas that channel the upslope and downslope flow. We used the forest condition-based flow map as our primary dataset and we boosted the score of cells if they were important for upslope, moisture/downslope, or poleward movement. To combine the circuitscape outputs, we z-scored the raw current flow values to put each grid on the same scale. To combine the three climate factors (upslope, moisture/downslope, and poleward) with the forest condition-based flow, we took the areas that were above-average (0.5 sd) for upslope, moisture/downslope, and poleward flow and overlaid each factor on the anthropogenic flow map and replaced the cell score if the cell score for the factor was higher. For example, a cell score of 1.2 for upslope would replace a northward anthropogenic flow score of 1.0, giving a slight bump-up to the cell reflecting its slope. If both factors had scores higher than the anthropogenic flow score, we replaced the latter with the highest score. This had the effect of raising the scores in areas with above-average current flow for upslope, moisture/downslope, or poleward movement but still retaining the geospatial forestcondition based regional flow score, and thus not penalizing areas for not having topographic climate relief options (Figures 27 and 28).

Classified Climate Flow Map

Areas that were added in as above average areas for upslope, moisture/downslope, or poleward were added as “Climate Flow” areas (diffuse flow (climate informed) and concentrated flow (climate informed linkage)).

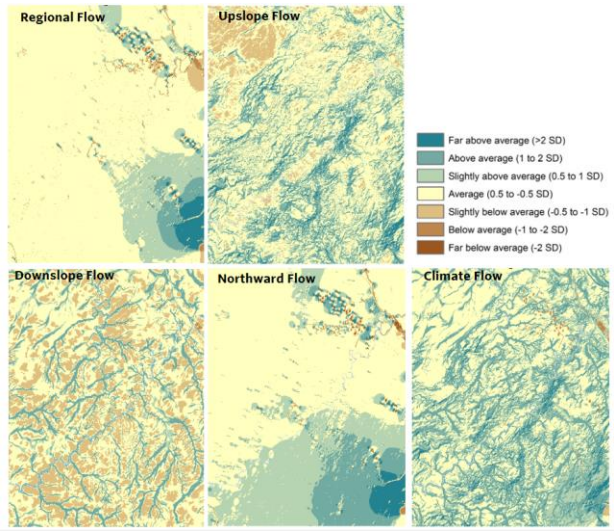

Figure 24: Integration of geospatial condition-based flow with upslope, downslope and northward flow to create the climate flow map. These maps for the Canyonlands region of Utah compare the results for regional flow based on anthropogenic resistance only with the climate flow that includes upslope flow, downslope flow, poleward flow, and integrated climate flow.

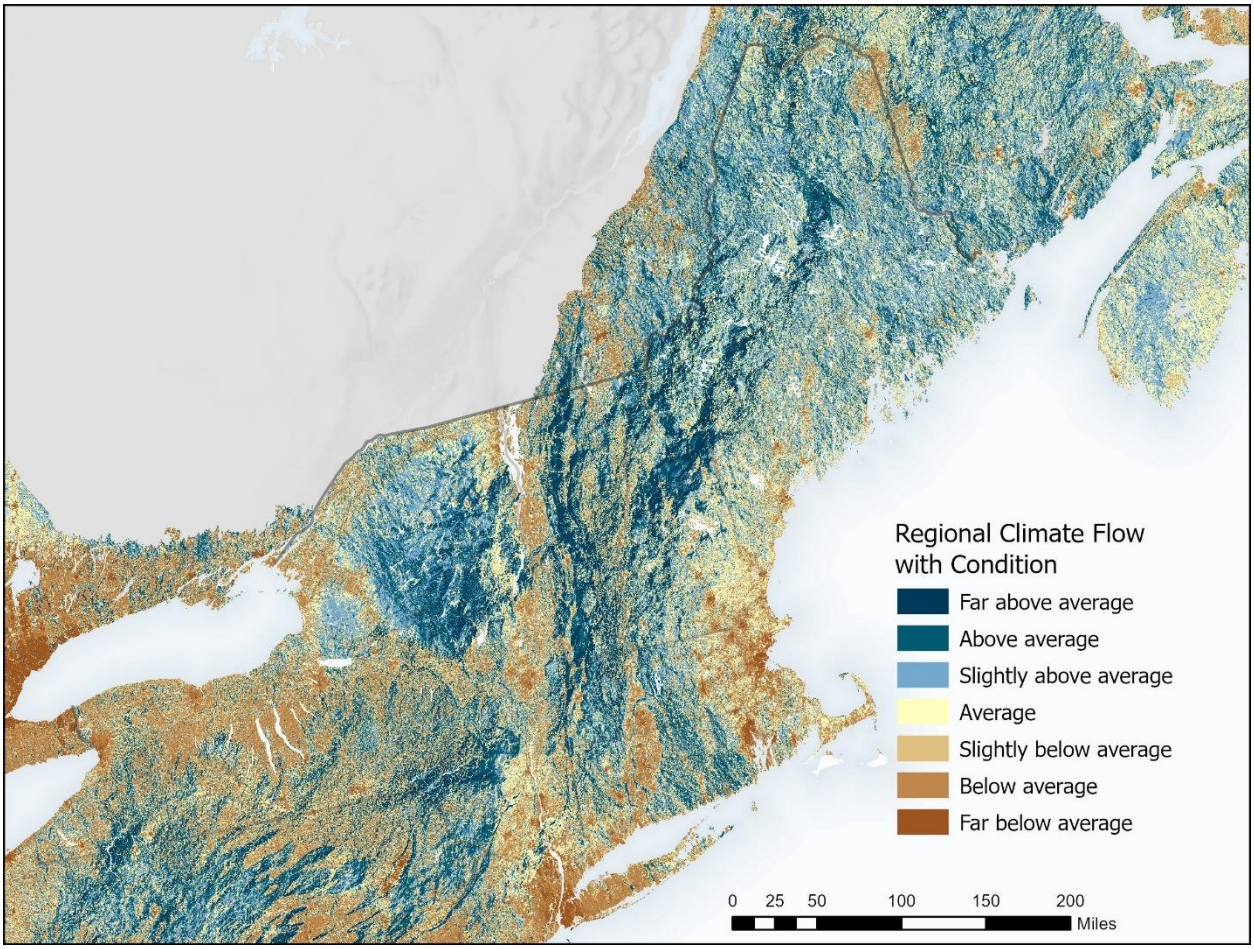

Figure 25: Regional Climate flow with Geospatial Forest Condition.

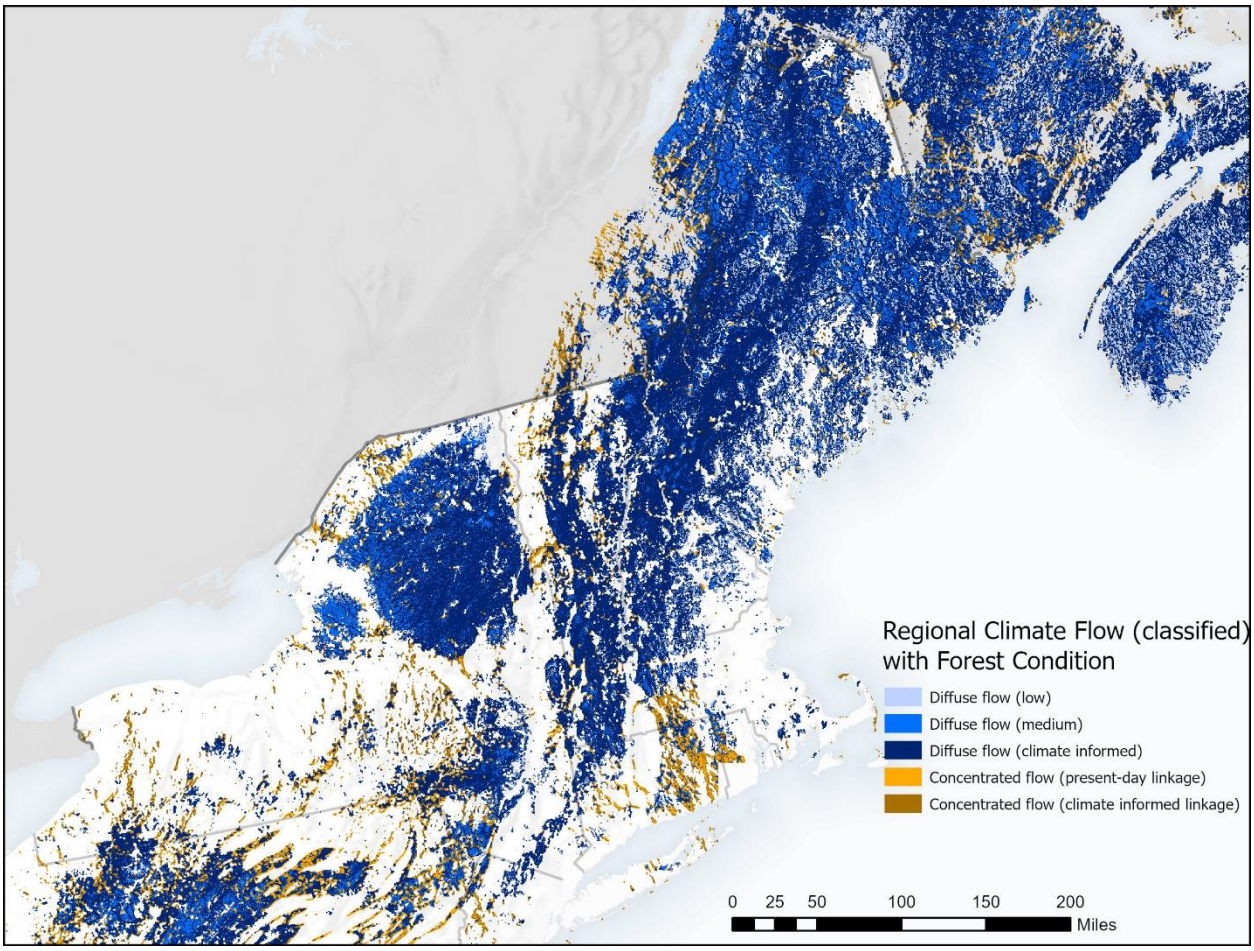

Figure 26: Classified Regional Climate flow with Geospatial Forest Condition.

Results and Discussion

Forest Distribution

The NSRC states are 76% forested for a total of 46 million acres. New York has the largest amount of forests with over 19 million acres and Maine has the largest amount of forests by percent (88%) (Figure 27). The dominant forest type is Northern Hardwood and Conifer with over 29 million acres, followed by Boreal Upland at 7.8 million acres and Central Oak-Pine at 2.9 million acres (Figure 28). The wetter parts of the landscape support 3.3 million acres of Northern Swamp and 600 thousand acres of Shrub Marsh.

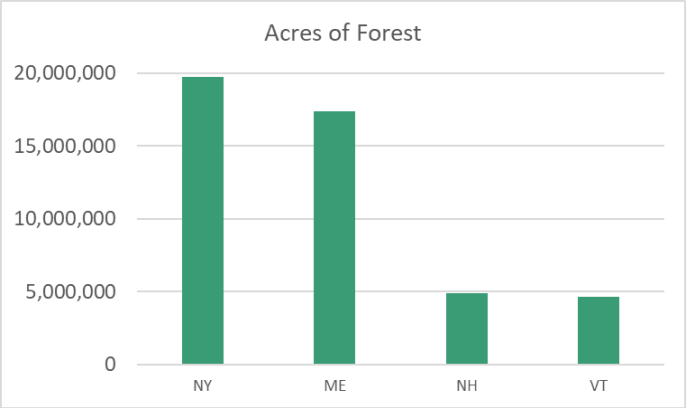

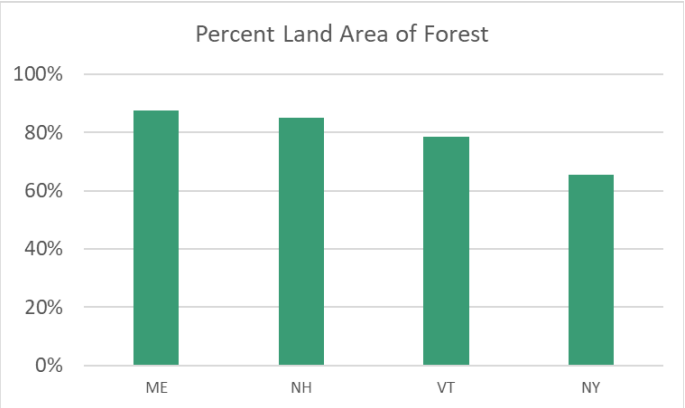

Figure 27: Forest Distribution by State.

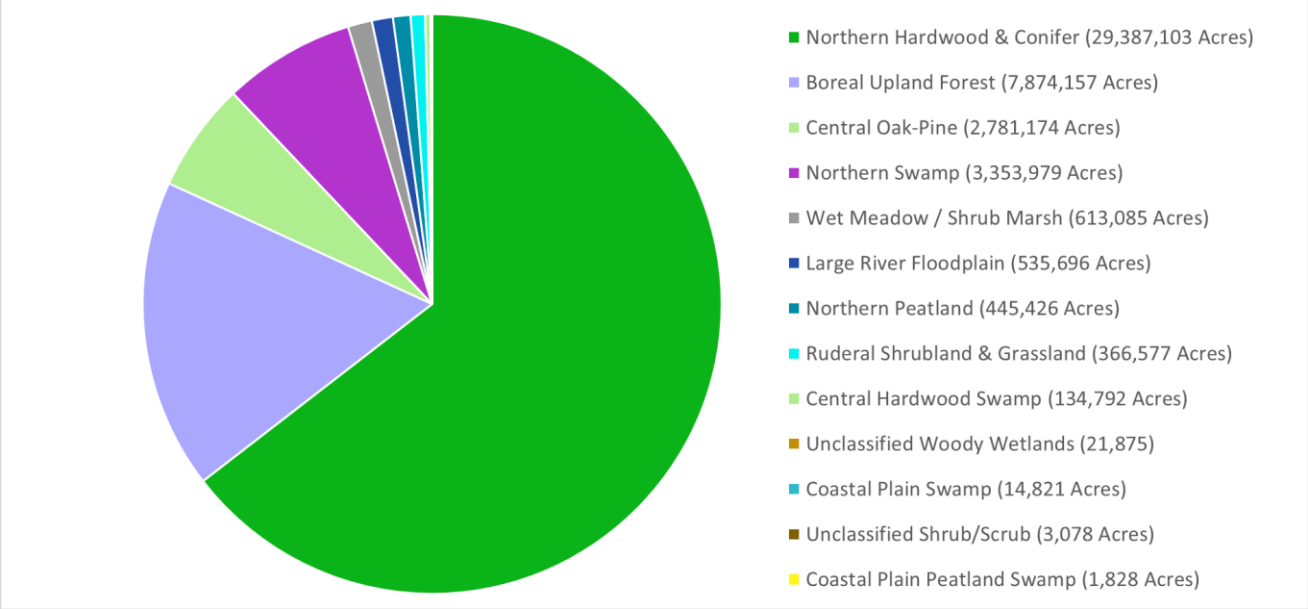

Figure 28: Acres of each Habitat Macrogroups in the NSRC states. Only habitats with over 1000 acres of total area are shown. The chart also includes three non-forest habitats: Wet Meadow/Shrub Marsh, Ruderal Shrubland and Grasslands, and Shrub/Scrub. The latter two are likely to be regrowing forest.

Forest Turnover

Over the last 23 years (2001-2023), 13% of the forest changed markedly. Over 3 million acres of non-forest returned to forest after being logged, cleared, or impacted by natural disturbance. The average rate of turnover across all forests and wetlands was 166,033 acres per year but it fluctuated between 90,000 to 230,000 acres per year (Figure 29). The rates were much higher for individual forest types. Northern Hardwood & Conifer Forest had the highest rate of turnover by area with an average of 80,000 acres per year (0.27%) followed by Boral Upland Forest at 53,000 acres per year. The latter, at 0.68%, was the highest rate by percentage of total forest. Central Oak-Pine at 1,900 acres per year (0.07%) had the least turnover by both measures (Figure 29, Table 5). Over the last 23 years, 13.7% of the forest land has returned to forest after a disturbance event. In contrast to turnover, only 0.5% of the forest was converted to development or industrial agriculture over the same 23 years. That indicates a conversion rate of 10,000 acres per year. Presumably these losses are long term or permanent.

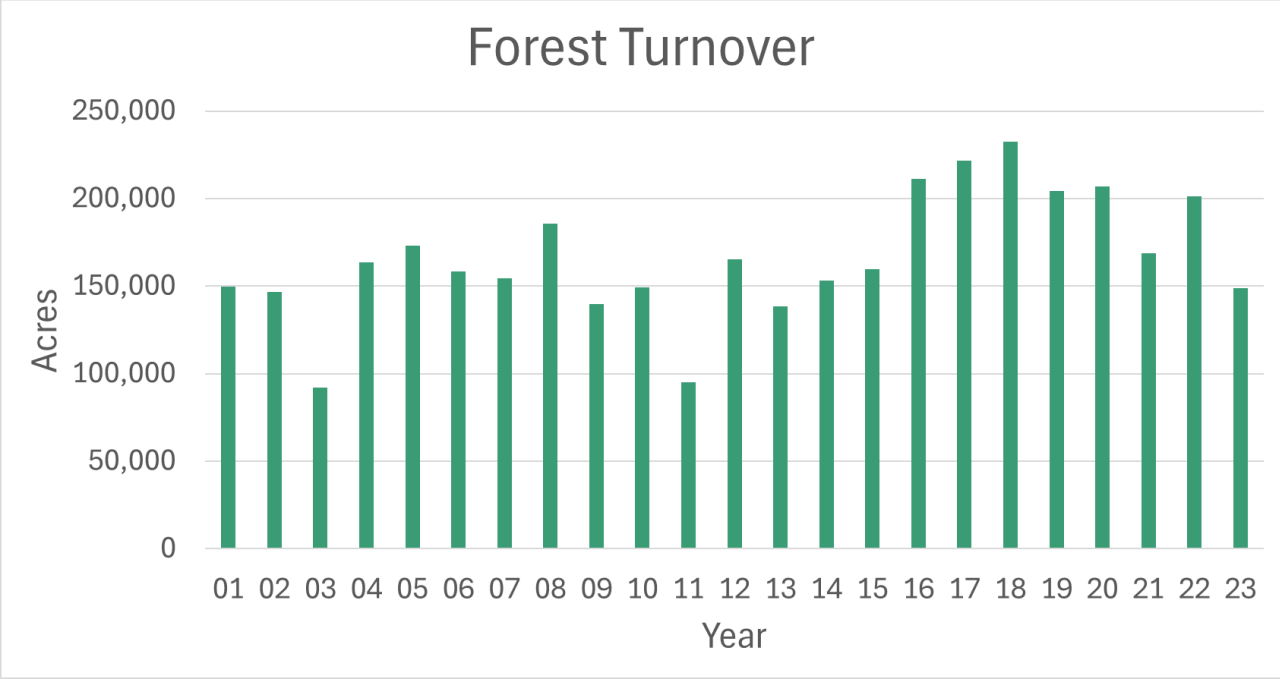

Figure 29: Average Forest Turnover Rate by Year.

Forest Type	Forest Turnover Annual Rate (acres per year)	Total Forest Acres	Percent Forest Turnover per Year
MATRIX FORMING FORESTS			
Central Oak-Pine	1,910	2,781,174	0.07%
Northern Hardwood & Conifer	80,697	29,387,103	0.27%
Boreal Upland Forest	53,498	7,874,157	0.68%
REGENERATING FORESTS			
Ruderal Shrubland & Grassland	188	366,577	0.05%
Shrub/Scrub	3	3,078	0.09%
Plantation and Ruderal Forest	2	724	0.28%
SWAMPS AND WETLAND FOREST			
Central Hardwood Swamp	84	134,792	0.06%
Coastal Plain Peat Swamp	1	1,828	0.07%
Coastal Plain Swamp	13	14,821	0.09%
Northern Peatland	424	445,426	0.10%
Woody Wetlands	22	21,875	0.10%
Large River Floodplain	561	535,696	0.10%
Northern Swamp	5,890	3,353,979	0.18%
NON-FOREST WETLANDS			
Wet Meadow / Shrub Marsh	541	613,085	0.09%

Table 5: Forest Turnover by Habitat Type

Forest Height

Matrix forming forests in the Northern States have an average height of 17.5 meters with a standard deviation of 4.9 meters. Central Oak-Pine has the highest average height at 19.9 meters and Norther Hardwood and Conifer is next highest with an average height of 18.6 meters (Table 6). The Ruderal Shrubland & Grasslands have the largest variation in height (SD = 6.42) showing the various stages of re-forestation and re-growth in this class.

Forest Type	Total Forest Acres	Mean Forest Height	STD Forest Height
MATRIX FORMING FORESTS			
Central Oak-Pine	2,781,174	19.91	5.13
Northern Hardwood & Conifer	29,387,103	18.62	4.90
Boreal Upland Forest	7,874,157	14.04	4.60
REGENERATING FORESTS			
Ruderal Shrubland & Grassland	366,577	16.89	6.46
Plantation and Ruderal Forest	724	14.26	5.33
SWAMPS AND WETLAND FOREST			
Coastal Plain Peat Swamp	1,828	18.28	4.87
Coastal Plain Swamp	14,821	17.55	5.24
Northern Swamp	3,353,979	16.25	5.59
Central Hardwood Swamp	134,792	16.24	5.92
Large River Floodplain	535,696	14.37	5.78
Northern Peatland	445,426	11.30	5.67
Woody Wetlands	21,875	9.85	7.13
NON-FOREST WETLANDS			
Wet Meadow / Shrub Marsh	613,085	13.73	6.20

Table 6. Forest Height by Macro-group

Anthropogenic Disturbance (Roads)

The three dominant forest types different markedly with respect to disturbance by roads. Boreal Upland Forest has the least amount of disturbance with a z-score of 1.1 SD above the average score for the region (0) (Figure 30). Northern Hardwoods and Conifer Forest were slightly above 0.5 SD while Central Oak-Pine Forest were slightly below 0 (-0.2 SD) reflecting their southern distribution in the more developed parts of the region. Swamps and wetlands varied widely with Northen Peatlands were the least disturbed (1.15 SD) while Coastal Plain Swamp was the most (-1.66 SD).

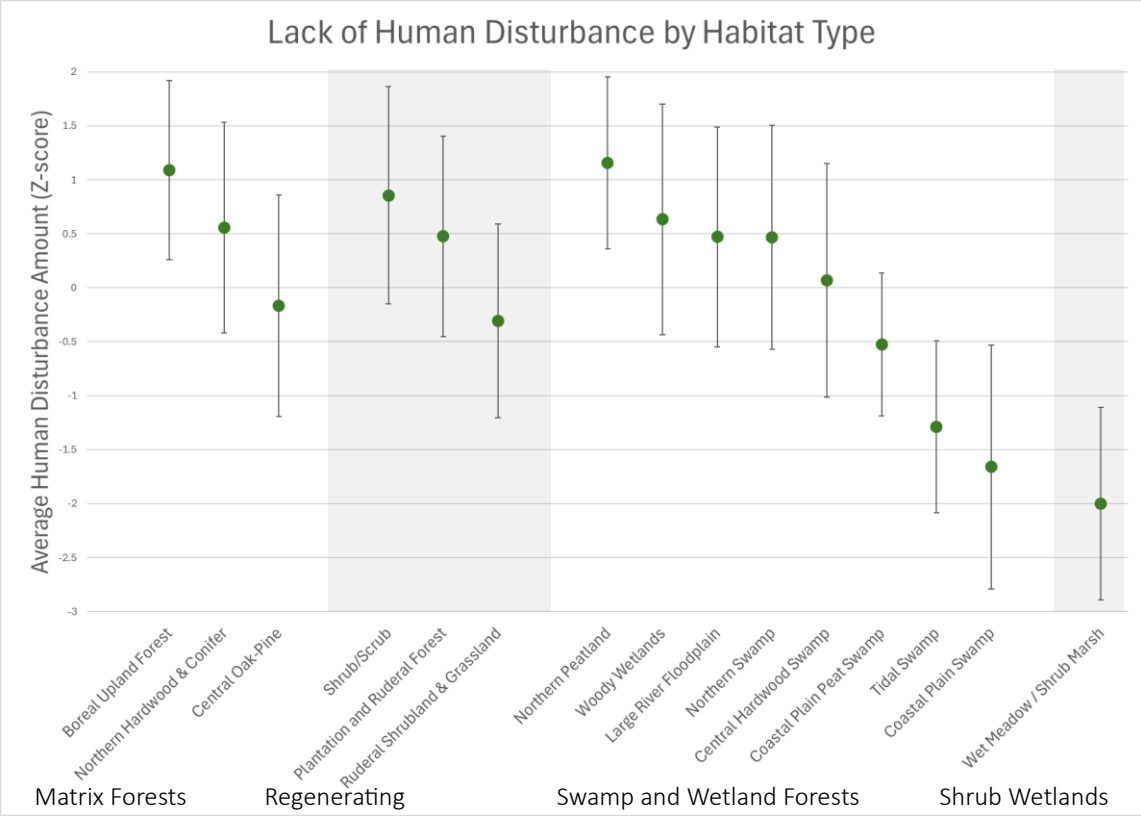

Figure 30: Lack of Human Disturbance by Habitat Type.

Geospatial Forest Condition Index

The integrated Geospatial Forest Condition Index allows users to evaluate individual condition attributes or the combined integrated metric at the site scale. When combining attributes we converted each metric to z-scores to ensure equal influence of forest turnover, forest height, and lack of human disturbance in the integrated metric. Note that the forest height metric was already relativized (z-scored) by habitat type due to the biological limits on growth for different species, and thus for summary stats the mean for height will always be zero for each habitat type.

Among the dominant forest types, all three are within the range of the mean (+/- 0.1 SD) although the Northern Hardwood and Conifer Forest is above zero while the other two are below zero. This suggests that when put on the same scale the rate of turnover offsets the lack of anthropogenic disturbance. The swamps and wetland are spread across the index with the Central Hardwood swamp, Northern Swamp, and the Large River Floodplain scoring relatively high while Coastal Plain Swamp and Tidal Swamp fall at the lowest end of the scale at almost 1 SD below the mean largely due to their high degree of human modification.

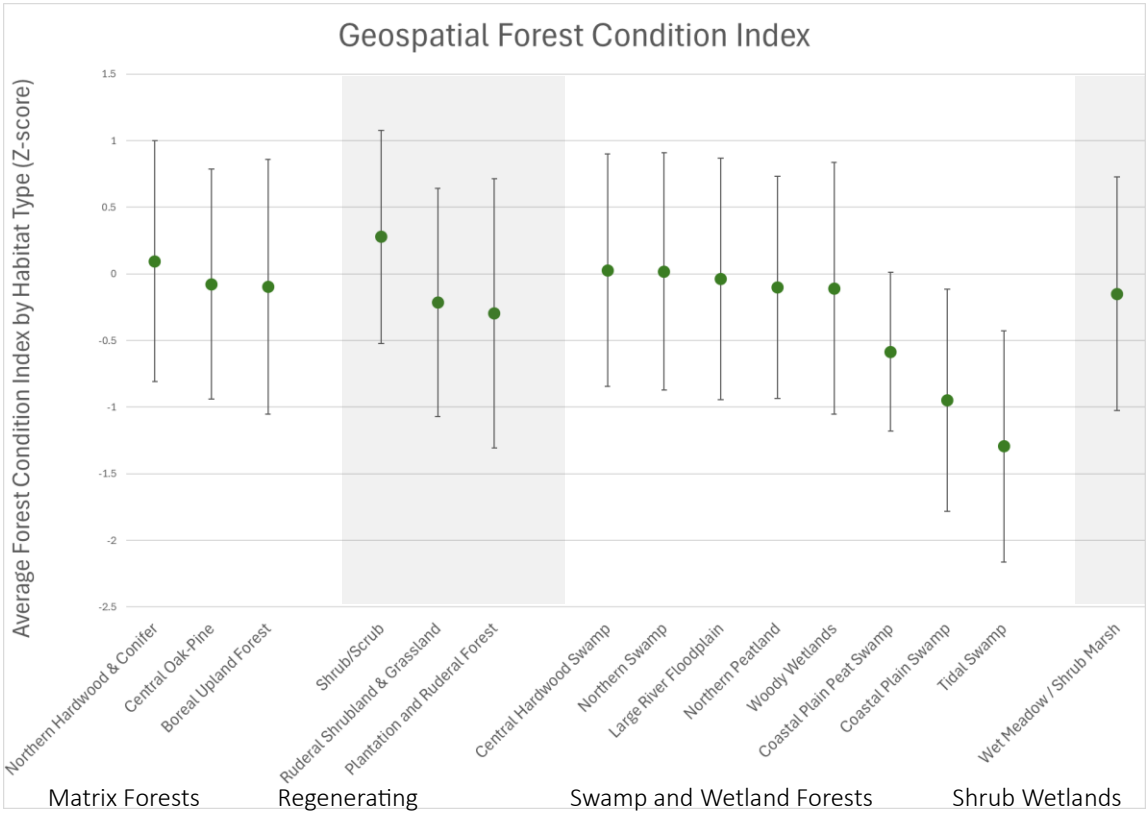

Figure 31: Forest Condition Index by Habitat Type

Connectivity for Range Shifts of Forests

For this study, we defined connectivity as a measure of habitat permeability based on the physical features and arrangement forest condition factors presumed to be important for forest organisms to move and sustain ecological processes. We focused on continuous, wall-to-wall permeability reflecting a goal of facilitating large-scale reorganization of species and habitats in response to climate change, which we suggest requires a comprehensive and continuous analysis: all organisms, in all directions, over many years. Thus, our aim was to create a model that reveals the implications of the landscape structure and condition with respect to the continuous flow of natural processes like range shifts, dispersal and recruitment.

Local Connectedness

Our first metric of connectivity was *Local connectedness*, starts with a focal cell and estimates the connectivity of flows outward from the cell in all directions within a three-kilometer local neighborhood. The resistance grid which the local connectedness was based off of anthropogenic landuse as well as the factors of forest condition. The local connectedness value is calculated as a Z-score, and when summarized for all forest types, the local connectedness value is 0.35 SD above the average for the region. Forests are, in general, have better connectedness than the surrounding landscape. Boral Upland Forests have the highest local connectedness value (+ 0.57 SD), followed by Northern Hardwood and Conifer (0.37 SD) (Figure 32). Central Oak Pine is the only major forest type below average (-.12 SD), due to this forest type being mostly in the more developed southern part of the region. The swamps and wetland are spread across the index with the Northern Peatland and the Northern Swamp scoring

relatively high while Coastal Plain Swamp and Tidal Swamp fall at the lowest end of the scale scoring below 1.5 SD below the mean largely due to their high degree of human modification.

While knowing the local connectedness value taking into account the current condition of forests is useful, knowing where improvements to forest condition can have the greatest benefit can help strategically plan forest management, conservation, and restoration. For this metric measured the difference between local connectedness with current forest condition and local connectedness with forests at their best possible condition. Across habitat types the total potential improvement types was similar (around 0.03 SD) (Figure 33). This suggests that focusing on the geographic location of improving condition is more important for change in local connectedness than forest type. Shrub/scrub, Plantations and Ruderal Forests, Central Hardwood Swamp, and Northern Swamp all have high standard deviations, indicate that in these habitat types there is a wide range of potential change in local connectedness with improved management, so identifying areas of high positive change could see outsized benefits in local connectedness.

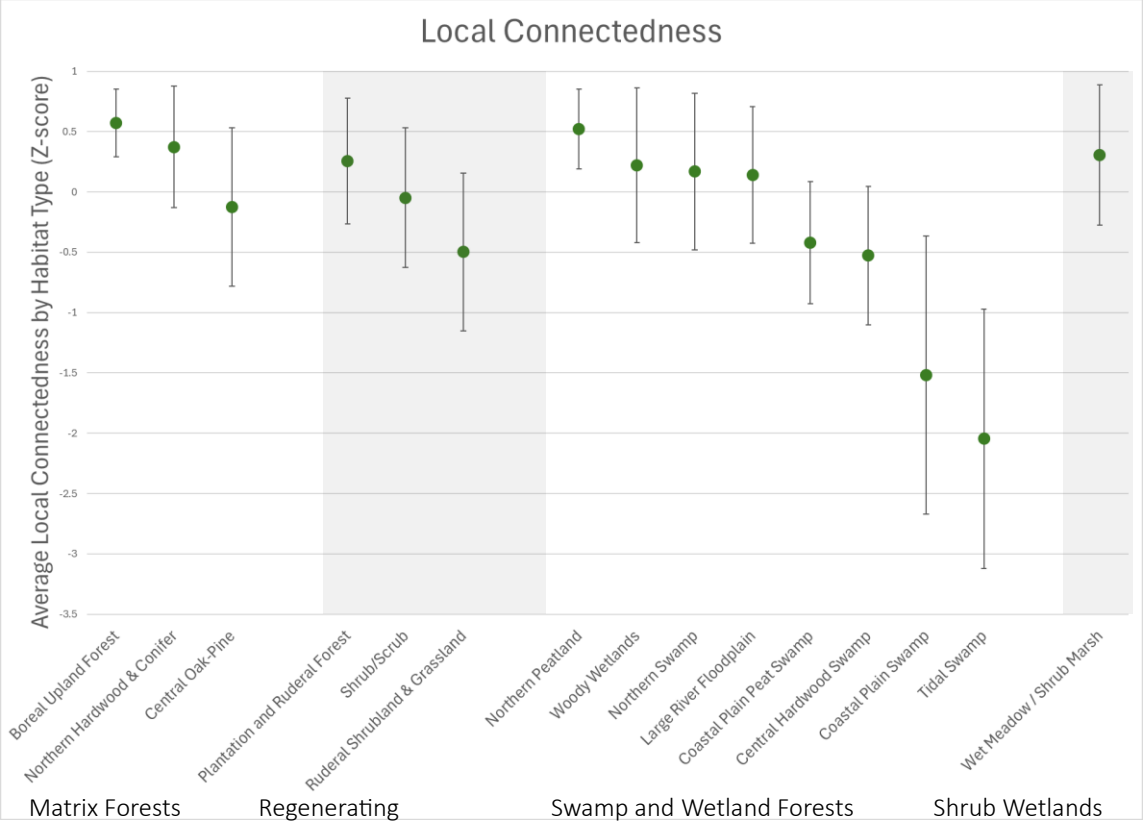

Figure 32: Local Connectedness by Habitat Type

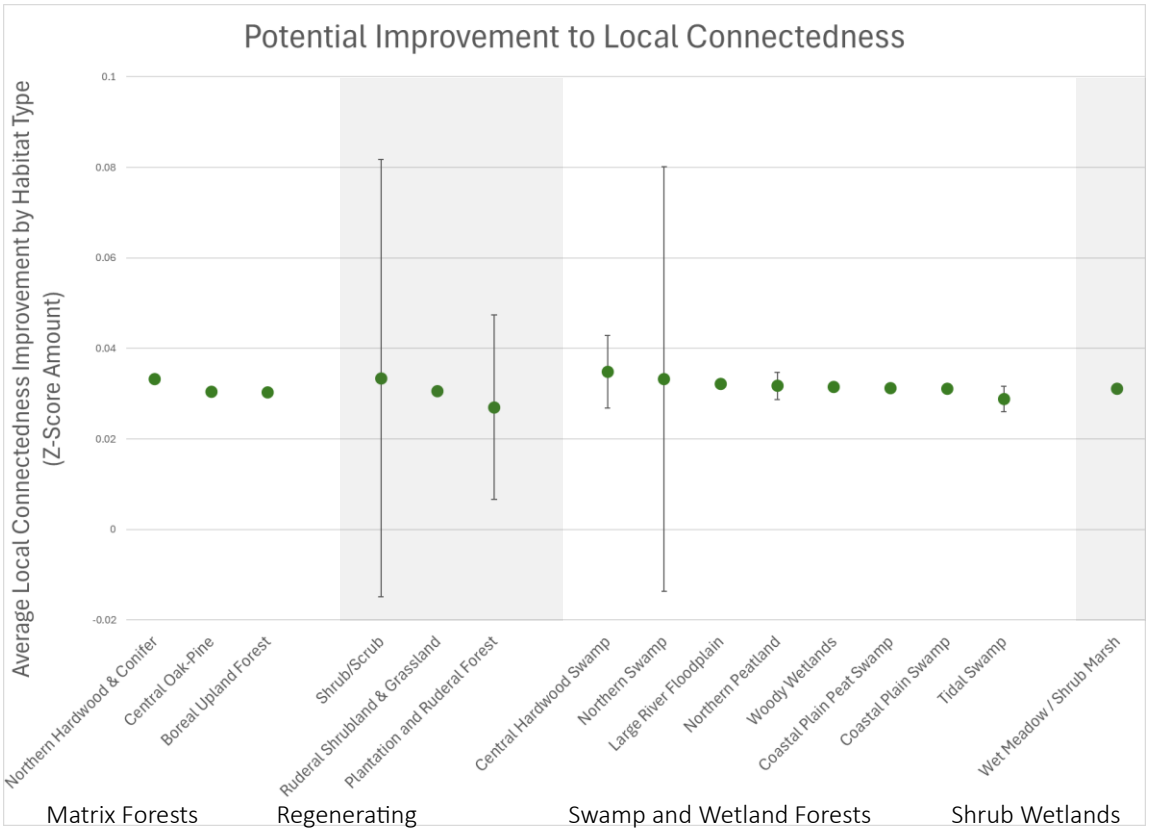

Figure 33: Potential Local Connectedness Improvement by Habitat Type

Regional Flow

Our second metric of connectivity was *Regional flow*, examines broad east-west and north-south flow patterns across the entire region. The results are a density of "current flow" in amps which is a proxy for natural movements and is function of its location, context, resistance, and direction of flow. Boral Upland Forests have the highest average regional flow value (12.2 amps), followed by Northern Hardwood and Conifer (12.14 amps) (Figure 34). Central Oak Pine has the lowest average regional flow (11.76 amps), due to this forest type being mostly in the more developed southern part of the region. The swamps and wetland are spread across the regional flow values with the Peatlands and the Large River Floodplain scoring relatively high while Coastal Plain Swamp and Tidal Swamp fall at the lowest end of the scale once again due to their high degree of human modification.

When looking at possible improvements to regional flow for range shifts with improved condition, the potential improvements follow the same trends as the overall regional flow. This indicated that the location of improved condition spatially is more important to take into consideration than the type of habitat. This is especially important in habitat groups with more variation in their values, like the Central Oak Pine, the regenerating forests, Coastal Plain Swam, and Tidal Swamp.

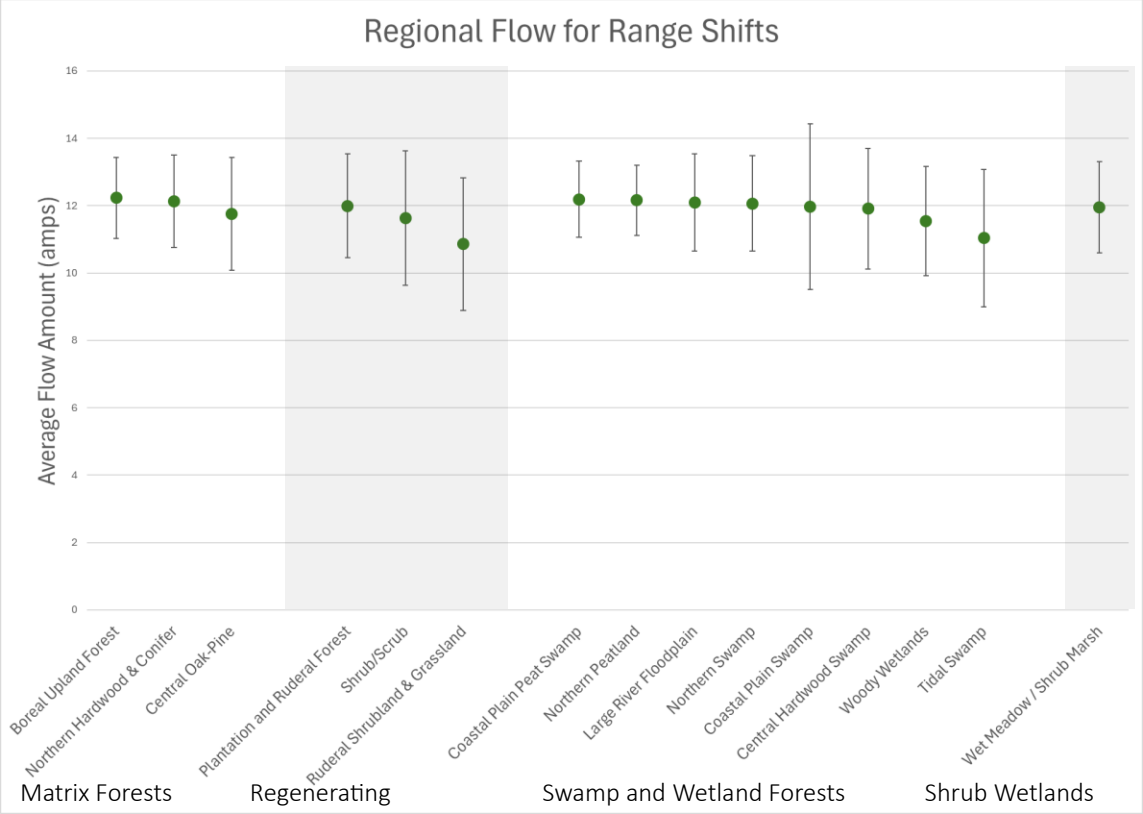

Figure 34: Regional Flow for Range Shifts by Habitat Type

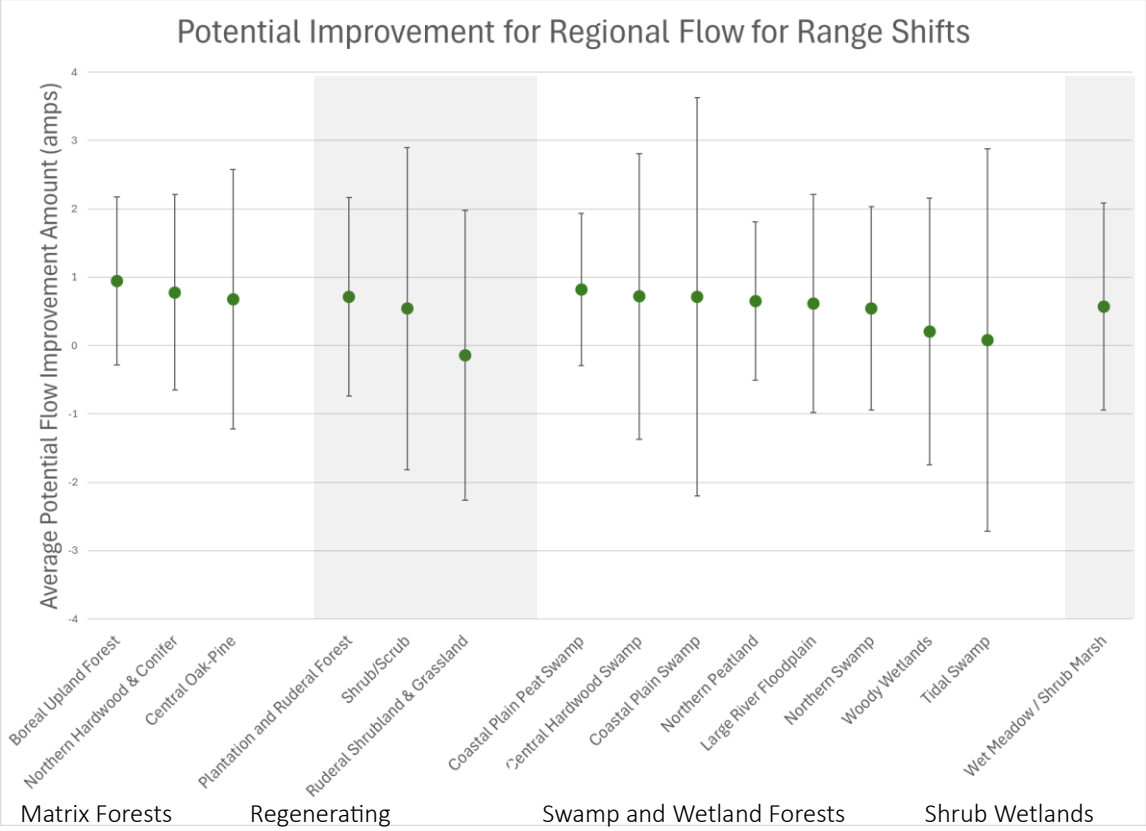

Figure 35: Potential Improvement in Regional Flow for Range Shifts by Habitat Type

References

Anderson, M., Clark, M., & Olivero, A. (2023). *Conservation Status of Natural Habitats in the Northeast*.

Anderson, M., Clark, M., Olivero Sheldon, A., Hall, K., Platt, J., Prince, J., Ahlering, M., & Cornett, M. (2018). *Resilient and Connected Landscapes for Terrestrial Conservation in the Central US.* https://tnc.app.box.com/s/50r22xaf7aaxhs5tx4ep1hsuc24pfg0c

Anderson, M. G., Clark, M. M., Olivero, A., & Prince, J. (2019). *Resilient Sites and Connected Landscapes for Terrestrial Conservation in the Rocky Mountain and Southwest Desert Region*. https://tnc.app.box.com/s/cqz4dp69e34mptqml7anfr5ezy94hcyu

Anderson, M. G., Clark, M., Olivero, A. P., Barnett, A. R., Hall, K. R., Cornett, M. W., Ahlering, M., Schindel, M., Unnasch, B., Schloss, C., & Cameron, D. R. (2023). A resilient and connected network of sites to sustain biodiversity under a changing climate. *Proceedings of the National Academy of Sciences*, *120*(7), e2204434119. https://doi.org/10.1073/pnas.2204434119

Anderson, M. G., Clark, M., & Sheldon, A. O. (2014). Estimating Climate Resilience for Conservation across Geophysical Settings. *Conservation Biology*, *28*(4), 959–970. https://doi.org/10.1111/cobi.12272

Avon, C., Bergès, L., Dumas, Y., & Dupouey, J. L. (2010). Does the effect of forest roads extend a few meters or more into the adjacent forest? A study on understory plant diversity in managed oak stands. *Forest Ecology and Management*, *259*(8). https://doi.org/10.1016/j.foreco.2010.01.031

Aylward, C. M., Murdoch, J. D., & Kilpatrick, C. W. (2020). Multiscale landscape genetics of American marten at their southern range periphery. *Heredity*, *124*(4), 550–561. https://doi.org/10.1038/s41437-020-0295-y

Balestrieri, A., Mori, E., Menchetti, M., Ruiz-González, A., & Milanesi, P. (2019). Far from the madding crowd: Tolerance toward human disturbance shapes distribution and connectivity patterns of closely related Martes spp. *Population Ecology*, *61*(3). https://doi.org/10.1002/1438-390X.12001

Barnett, K., & Belote, R. T. (2021). Modeling an aspirational connected network of protected areas across North America. *Ecological Applications*, *31*(6). https://doi.org/10.1002/EAP.2387

Bechtold, W. A., & Patterson, P. L. (2005). The Enhanced Forest Inventory and Analysis Program — National Sampling Design and Estimation Procedures. *USDA General Technical Report*, *SRS-80*.

Beier, P. (2012). Conceptualizing and designing corridors for climate change. *Ecological Restoration*, *30*(4), 312–319. https://doi.org/10.3368/er.30.4.312

Belote, R. T., Barnett, K., Zeller, K., Brennan, A., & Gage, J. (2022). Examining local and regional ecological connectivity throughout North America. *Landscape Ecology*, *37*(12). https://doi.org/10.1007/s10980-022-01530-9

Bolster, C. H., Mitchell, R., Kitts, A., Campbell, A., Cosh, M., Farrigan, T. L., Franzluebbers, A. J., Hoover, D. L., Jin, V. L., Peck, D. E., Schmer, M. R., & Smith, M. D. (2024). Fifth National Climate Assessment Released. *CSA News*, *69*(1). https://doi.org/10.1002/csan.21194

Botkin, D. B., Saxe, H., Araújo, M. B., Betts, R., Bradshaw, R. H. W., Cedhagen, T., Chesson, P., Dawson, T. P., Etterson, J. R., Faith, D. P., Ferrier, S., Guisan, A., Hansen, A. S., Hilbert, D. W., Loehle, C.,

Margules, C., New, M., Sobel, M. J., & Stockwell, D. R. B. (2007). Forecasting the Effects of Global Warming on Biodiversity. *BioScience*, *57*(3), 227–236. https://doi.org/10.1641/B570306

(CCRS), C. C. for R. S. (2020). *2020 Land Cover of Canada*. North American Land Change Monitoring System (NALCMS).

Chen, I. C., Hill, J. K., Ohlemüller, R., Roy, D. B., & Thomas, C. D. (2011). Rapid range shifts of species associated with high levels of climate warming. *Science*, *333*(6045), 1024–1026. https://doi.org/10.1126/science.1206432

Compton, B. W., McGarigal, K., Cushman, S. A., & Gamble, L. R. (2007). A resistant-kernel model of connectivity for amphibians that breed in vernal pools. *Conservation Biology*, *21*(3), 788–799. https://doi.org/10.1111/j.1523-1739.2007.00674.x

Crimmins, S. M., Dobrowski, S. Z., Greenberg, J. A., Abatzoglou, J. T., & Mynsberge, A. R. (2011). Changes in climatic water balance drive downhill shifts in plant species' optimum elevations. *Science*, *331*(6015), 324–327. https://doi.org/10.1126/science.1199040

Dawson, T. P., Jackson, S. T., House, J. I., Prentice, I. C., & Mace, G. M. (2011). Beyond Predictions: Biodiversity Conservation in a Changing Climate. *Science*, *332*(6025), 53–58. http://10.0.4.102/science.1200303

Dewitz, J., & USGS. (2023). National Land Cover Database (NLCD) 2021 Products. In *U.S. Geological Survey data release*. Earth Resources Observation and Science (EROS) Center.

Dickson, B. G., Albano, C. M., Anantharaman, R., Beier, P., Fargione, J., Graves, T. A., Gray, M. E., Hall, K. R., Lawler, J. J., Leonard, P. B., Littlefield, C. E., McClure, M. L., Novembre, J., Schloss, C. A., Schumaker, N. H., Shah, V. B., & Theobald, D. M. (2019). Circuit-theory applications to connectivity science and conservation. In *Conservation Biology* (Vol. 33, Issue 2, pp. 239–249). Blackwell Publishing Inc. https://doi.org/10.1111/cobi.13230

Dobrowski, S. Z. (2011). A climatic basis for microrefugia: The influence of terrain on climate. In *Global Change Biology* (Vol. 17, Issue 2, pp. 1022–1035). https://doi.org/10.1111/j.1365-2486.2010.02263.x

Dobrowski, S. Z., & Parks, S. A. (2016). Climate change velocity underestimates climate change exposure in mountainous regions. *Nature Communications*, *7*(1), 12349. https://doi.org/10.1038/ncomms12349

Fei, S., Desprez, J. M., Potter, K. M., Jo, I., Knott, J. A., & Oswalt, C. M. (2017). Divergence of species responses to climate change. *Science Advances*, *3*(5), e1603055. https://doi.org/10.1126/sciadv.1603055

Ferrari, I., & Ferrarini, A. (2008). From ecosystem ecology to landscape ecology: A progression calling for a well-founded research and appropriate disillusions. *Landscape Online*, *6*(1). https://doi.org/10.3097/LO.200806

Ferree, C. E., & Anderson, M. G. (2013). A map of terrestrial habitats of the Northeastern United States: Methods and approach. In *Nature Conservancy*.

Forman, R. T. T. (2003). Road Ecology: Science and solutions. In *Environmental Progress* (Vol. 22, Issue 3). Island Press. https://doi.org/10.1002/ep.670220307

Forman, R. T. T., & Godron, M. (1986). *Landscape Ecology*. John Wiley and Sons Ltd.

Foster, D., Donahue, B., Faison, E., Howell, L., Hunter, M., Irland, L., Leibowitz, J., Masino, S., Orwid, D., Perschel, R., Publicover, D., Sayen, J., Sferra, N., Thompson, E., & Thompson, J. (2023). *Wildlands of New England 2022 GIS Polygons*. Harvard Forest.

Foster, D., Donahue, B. M., Kittredge, D. B., Lambert, K., Hunter, M. L., Hall, B., Irland, L., Lilieholm, R., Orwig, D., D'Amato, A., Colburn, E. A., Thompson, J. R., Levitt, J. N., Ellison, A. M., Keeton, W., Aber, J., Cogbill, C. V, Driscoll, C., Fahey, T. J., & Hart, C. (2010). *Wildland and woodlands: a vision for the New England landscape*. Harvard University Press.

Fractracker Alliance. (2024). *National Energy and Petrochemical Map*. https://www.fractracker.org/map/national/

Gawler, S. C. (2008). Northeastern terrestrial wildlife habitat classification. In *Report to the Virginia Department of Game and Inland Fisheries on behalf of the Northeast Association of Fish and Wildlife Agencies and the National Fish and Wildlife Foundation* (Issue November).

Geofabrik, D. S. (2022a). *Open Street Map*. Geofabrik Download Server.

Geofabrik, D. S. (2022b). *Open Street Map*. Geofabrik Download Server.

Grantham, H. S., Duncan, A., Evans, T. D., Jones, K. R., Beyer, H. L., Schuster, R., Walston, J., Ray, J. C., Robinson, J. G., Callow, M., Clements, T., Costa, H. M., DeGemmis, A., Elsen, P. R., Ervin, J., Franco, P., Goldman, E., Goetz, S., Hansen, A., … Watson, J. E. M. (2020). Anthropogenic modification of forests means only 40% of remaining forests have high ecosystem integrity. *Nature Communications*, *11*(1). https://doi.org/10.1038/s41467-020-19493-3

Groffman, P. M., Rustad, L. E., Templer, P. H., Campbell, J. L., Christenson, L. M., Lany, N. K., Socci, A. M., Vadeboncoeur, M. A., Schaberg, P. G., Wilson, G. F., Driscoll, C. T., Fahey, T. J., Fisk, M. C., Goodale, C. L., Green, M. B., Hamburg, S. P., Johnson, C. E., Mitchell, M. J., Morse, J. L., … Rodenhouse, N. L. (2012). Long-Term Integrated Studies Show Complex and Surprising Effects of Climate Change in the Northern Hardwood Forest. *BioScience*, *62*(12), 1056–1066. https://doi.org/10.1525/BIO.2012.62.12.7

Hall, K. R., Anantharaman, R., Landau, V. A., Clark, M., Dickson, B. G., Jones, A., Platt, J., Edelman, A., & Shah, V. B. (2021). Circuitscape in Julia: empowering dynamic approaches to connectivity assessment. *Land*, *10*(3). https://doi.org/10.3390/land10030301

Hansen, M. C., Potapov, P. V., Moore, R., Hancher, M., Turubanova, S. A., Tyukavina, A., Thau, D., Stehman, S. V., Loveland, T. R., Kommareddy, A., Egorov, A., Chini, L., Justice, C. O., & Townshend, J. R. G. (2013). High-Resolution Global Maps of 21st-Century Forest Cover Change. *Science*, *342*(6160), 850–853. https://doi.org/10.1126/science.1244693

Heller, N. E., & Zavaleta, E. S. (2009). Biodiversity management in the face of climate change: A review of 22 years of recommendations. *Biological Conservation*, *142*(1), 14–32. https://doi.org/10.1016/j.biocon.2008.10.006

Hersteinsson, P., & MacDonald, D. W. (1992). Interspecific Competition and the Geographical Distribution of Red and Arctic Foxes Vulpes Vulpes and Alopex lagopus. *Oikos*, *64*(3), 505–515. https://doi.org/10.2307/3545168

Hilty, J. A., & Possingham, H. (2019). *Corridor ecology : linking landscapes for biodiversity conservation and climate adaptation* (Second edi). Island Press.

Hitch, A. T., & Leberg, P. L. (2007). Breeding distributions of North American bird species moving north as a result of climate change. *Conservation Biology*, *21*(2), 534–539. https://doi.org/10.1111/j.1523-1739.2006.00609.x

Hoen, B. D., Diffendorfer, J. E., Rand, J. T., Kramer, L. A., Garrity, C. P., & Hunt, H. E. (2022). *United States Wind Turbine Database ver. 7.0*. U.S. Geological Survey, American Clean Power Association, and Lawrence Berkeley National Laboratory Data Release,. https://doi.org/https://doi.org/10.5066/F7TX3DN0.

Holland, I., & Meyer, S. (2018). *The Economic Case for Conservation: A Synthesis of the Economic Impacts of Natural Resources and Conservaiton in New England*.

Hoover, C. M., Bartig, J. L., Bogaczyk, B., Breeden, C., Iverson, L. R., Prout, L., & Sheffield, R. M. (2022). Forest inventory and analysis data in action: Examples from eastern national forests. *Trees, Forests and People*, *7*. https://doi.org/10.1016/j.tfp.2021.100178

Hunter, M., Gibbs, J., & Popescu, B. (2021). *Fundamentals of Conservation Biology*.

Iverson, L. R., & McKenzie, D. (2013). Tree-species range shifts in a changing climate: Detecting, modeling, assisting. *Landscape Ecology*, *28*(5). https://doi.org/10.1007/s10980-013-9885-x

Iverson, L. R., Prasad, A., & Schwartz, M. W. (1999). Modeling potential future individual tree-species distributions in the eastern united states under a climate change scenario: A case study with Pinus virginiana. *Ecological Modelling*, *115*(1). https://doi.org/10.1016/S0304-3800(98)00200-2

Iverson, L. R., Schwartz, M. W., & Prasad, A. M. (2004). How fast and far might tree species migrate in the eastern United States due to climate change? *Global Ecology and Biogeography*, *13*(3). https://doi.org/10.1111/j.1466-822X.2004.00093.x

Knight, A. T., Cowling, R. M., Difford, M., & Campbell, B. M. (2010). Mapping human and social dimensions of conservation opportunity for the scheduling of conservation action on private land. *Conservation Biology*, *24*(5), 1348–1358. https://doi.org/10.1111/j.1523-1739.2010.01494.x

Kosiba, A. (2023). *Building the New Forest Future - Ensuring Long-Term Forest Health and Resiliency*.

KROSBY, M., TEWKSBURY, J., HADDAD, N. M., & HOEKSTRA, J. (2010). Ecological Connectivity for a Changing Climate. *Conservation Biology*, *24*(6), 1686–1689. https://doi.org/10.1111/j.1523-1739.2010.01585.x

Kuhn, E., & Gégout, J. C. (2019). Highlighting declines of cold-demanding plant species in lowlands under climate warming. *Ecography*, *42*(1), 36–44. https://doi.org/10.1111/ECOG.03469/FORMAT/PDF

LaPoint, E. (2005). Access and use of FIA data through FIA spatial data services. *Proceedings of the Fifth Annual Forest Inventory and Analysis Symposium*.

Loarie, S. R., Duffy, P. B., Hamilton, H., Asner, G. P., Field, C. B., & Ackerly, D. D. (2009). The velocity of climate change. *Nature*, *462*(7276), 1052–1055. https://doi.org/10.1038/nature08649

Lynch, J. F., & Whigham, D. F. (1984). Effects of forest fragmentation on breeding bird communities in Maryland, USA. *Biological Conservation*, *28*(4). https://doi.org/10.1016/0006-3207(84)90039-9

Magioli, M., Bovo, A. A. A., Huijser, M. P., Abra, F. D., Miotto, R. A., Andrade, V. H. V. P., Nascimento, A. M., Martins, M. Z. A., & Ferraz, K. M. P. M. de B. (2019). Short and narrow roads cause substantial impacts on wildlife. *Oecologia Australis*, *23*(1). https://doi.org/10.4257/OECO.2019.2301.09

McGarigal, K., Compton, B. W., Plunkett, E. B., DeLuca, W. V, Grand, J., Ene, E., & Jackson, S. D. (2018). A landscape index of ecological integrity to inform landscape conservation. *Landscape Ecology*, *33*(7), 1029–1048. https://doi.org/10.1007/s10980-018-0653-9

Mikołajczyk, T., & Nawrocki, P. (2019). Forest management practices and the occurrence of suspended solids in rivers and streams and their influence on ichthyofauna and river ecosystems. *Forest Research Papers*, *80*(4). https://doi.org/10.2478/frp-2019-0027

Moritz, C., Patton, J. L., Conroy, C. J., Parra, J. L., White, G. C., & Beissinger, S. R. (2008). Impact of a century of climate change on small-mammal communities in Yosemite National Park, USA. *Science*, *322*(5899), 261–264. https://doi.org/10.1126/science.1163428

Olson, D. H., Anderson, P. D., Frissell, C. A., Welsh, H. H., & Bradford, D. F. (2007). Biodiversity management approaches for stream–riparian areas: Perspectives for Pacific Northwest headwater forests, microclimates, and amphibians. *Forest Ecology and Management*, *246*(1), 81–107. https://doi.org/https://doi.org/10.1016/j.foreco.2007.03.053

Parmesan, C., Ryrholm, N., Stefanescu, C., Hill, J. K., Thomas, C. D., Descimon, H., Huntley, B., Kaila, L., Kullberg, J., Tammaru, T., Tennent, W. J., Thomas, J. A., & Warren, M. (1999). Poleward shifts in geographical ranges of butterfly species associated with regional warming. *Nature*, *399*(6736), 579–583. https://doi.org/10.1038/21181

Parmesan, C., & Yohe, G. (2003a). A globally coherent fingerprint of climate change impacts across natural systems. *Nature*, *421*(6918), 37–42. https://doi.org/10.1038/nature01286

Parmesan, C., & Yohe, G. (2003b). *A globally coherent fingerprint of climate change impacts across natural systems*. www.nature.com/nature

Pelletier, D., Clark, M., Anderson, M. G., Rayfield, B., Wulder, M. A., & Cardille, J. A. (2014). Applying circuit theory for corridor expansion and management at regional scales: Tiling, pinch points, and omnidirectional connectivity. *PLoS ONE*, *9*(1), e84135. https://doi.org/10.1371/journal.pone.0084135

Poldrack, R. (2023). *8.10: Z-scores*. Statistics LibreTexts .

Potapov, P., Li, X., Hernandez-Serna, A., Tyukavina, A., Hansen, M. C., Kommareddy, A., Pickens, A., Turubanova, S., Tang, H., Silva, C. E., Armston, J., Dubayah, R., Blair, J. B., & Hofton, M. (2021). Mapping global forest canopy height through integration of GEDI and Landsat data. *Remote Sensing of Environment*, *253*. https://doi.org/10.1016/j.rse.2020.112165

Pounds, J. A., Fogden, M. P. L., & Campbell, J. H. (1999). Biological response to climate change on a tropical mountain. *Nature*, *398*(6728), 611–615. https://doi.org/10.1038/19297

Schoen, J. M., Neelakantan, A., Cushman, S. A., Dutta, T., Habib, B., Jhala, Y. V., Mondal, I., Ramakrishnan, U., Reddy, P. A., Saini, S., Sharma, S., Thatte, P., Yumnam, B., & DeFries, R. (2022). Synthesizing habitat connectivity analyses of a globally important human-dominated tiger-conservation landscape. *Conservation Biology*, *36*(4). https://doi.org/10.1111/cobi.13909

Shah, V. B., & McRae, B. (2008). Circuitscape: A Tool for Landscape Ecology. In G. Varoquaux, T. Vaught, & J. Millman (Eds.), *Proceedings of the 7th Python in Science Conference* (pp. 62–65).

Small, R. A., & Lewis, D. J. (2010). Forest land conversion, ecosystem services, and economic issues for policy: A review. In *Forest Fragmentation and Land Conversion: Analysis of Select Issues*.

Smith, R. I. L. (1994). Vascular Plants as Bioindicators of Regional Warming in Antarctica. *Oecologia*, *99*(3/4), 322–328. http://www.jstor.org/stable/4220764

Sturm, M., Racine, C., & Tape, K. (2001). Increasing shrub abundance in the Arctic. *Nature*, *411*(6837), 546–547. https://doi.org/10.1038/35079180

Theobald, D. M., Keeley, A. T. H., Laur, A., & Tabor, G. (2022). A simple and practical measure of the connectivity of protected area networks: The ProNet metric. *Conservation Science and Practice*, *4*(11), e12823. https://doi.org/https://doi.org/10.1111/csp2.12823

Trombulak, S. C., & Frissell, C. A. (2000). Review of ecological effects of roads on terrestrial and aquatic communities. *Conservation Biology*, *14*(1). https://doi.org/10.1046/j.1523-1739.2000.99084.x

U.S. Census Bureau. (2023). *Tiger Line Shapefiles*. U.S. Department of Commerce, Geography Division, U.S. Census Bureau. https://www.census.gov/geographies/mapping-files/time-series/geo/tiger-line-file.html

U.S. EPA. (2024). *Emissions and Generation Resource Integrated Database (eGRID2010)*. https://www.epa.gov/energy/emissions-generation-resource-integrated-database-egrid

U.S. Geological Survey. (2019). *1 arc-second Digital Elevation Models (DEMs) - USGS National Map 3DEP*. U.S. Geological Survey.

USDA Farm Services Agency. (2019). *NAIP on AWS - Registry of Open Data on AWS*. https://registry.opendata.aws/naip/

van Herk, C. M., Aptroot, A., & van Dobben, H. F. (2002). Long-Term Monitoring in the Netherlands Suggests that Lichens Respond to Global Warming. *The Lichenologist*, *34*(2), 141–154. https://doi.org/DOI: 10.1006/lich.2002.0378

Zeller, K. A., McGarigal, K., & Whiteley, A. R. (2012). Estimating landscape resistance to movement: A review. In *Landscape Ecology* (Vol. 27, Issue 6). https://doi.org/10.1007/s10980-012-9737-0

Zhou, D., Liu, S., Oeding, J., & Zhao, S. (2013). Forest cutting and impacts on carbon in the eastern United States. *Scientific Reports*, *3*. https://doi.org/10.1038/srep03547

Zuckerberg, B., Woods, A. M., & Porter, W. F. (2009). Poleward shifts in breeding bird distributions in New York State. *Global Change Biology*, *15*(8), 1866–1883. https://doi.org/10.1111/j.1365-2486.2009.01878.x